undetectable: the values (pg/mL) were 3.39 ± 4.70 on day 3 after treatment and 2.77 ± 3.30 on day 7 for the SAL group and 16.39 ± 5.83 on day 3 and 8.26 ± 2.23 on day 7 for the injection group. The hydrogel group exhibited apparently higher concentrations of BDNF on days 3 and 7 compared with the other experimental groups: the values were 675.00 ± 230.22 on day 3 and 884.77 ± 100.35 on day 7 (Fig. 1). The overall effect of the experimental groups on BDNF concentrations were statistically significant ($P <$ .0001). Significant differences were also detected in the BDNF concentrations on days 3 and 7 between the SAL and gel groups and between the injection and gel groups.

Functional Protection

The eABR threshold on day 18 after KM and EA treatment (before drug application) was 0.727 ± 0.092 mA. The SAL group exhibited an obvious elevation of the eABR threshold over time: the values (mA) were 0.960 ± 0.079 on day 3 and 0.992 ± 0.073 on day 7 (Fig. 2). By contrast, no significant elevation of the threshold was detected in the BDNF group: the values were 0.745 ± 0.067 on day 3 and 0.760 ± 0.073 on day 7 (Fig. 2). The overall effect of the experimental groups on elevation of the eABR threshold was statistically significant ($P <$ .0001). Significant differences were also detected in the thresholds on day 3 or 7 between the SAL and BDNF groups. The thresholds of the SAL group on days 3 and 7 were significantly higher than those before drug application, whereas no significant differences were detected after BDNF application. These findings indicate that the application of BDNF by way of the biodegradable hydrogel maintained the functionality of the SGNs.

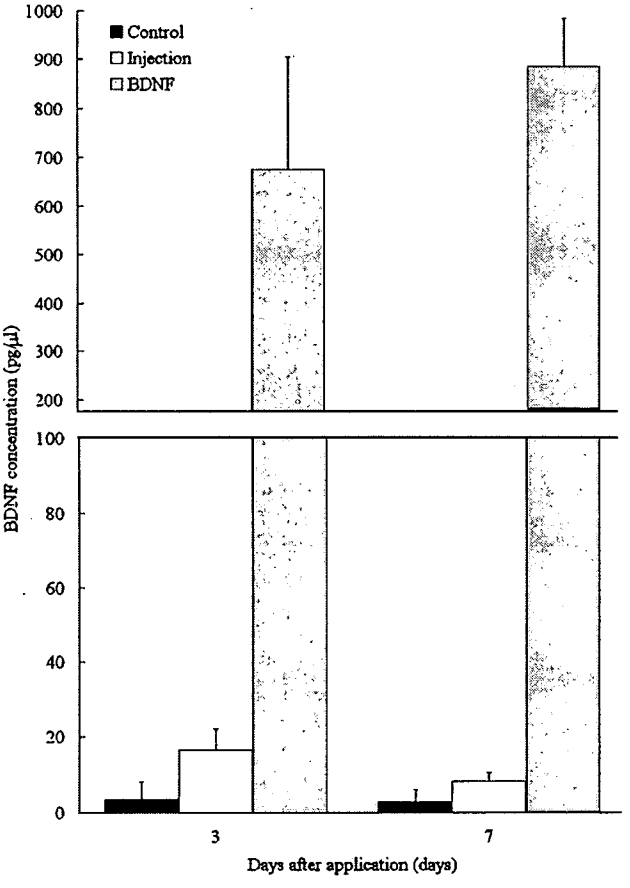

Fig. 1. Brain-derived neurotrophic factor (BDNF) concentrations in the perilymph 3 or 7 days after BDNF application by hydrogel, single injection, or no treatment. Bars on left show BDNF concentrations in the perilymph without treatment (control group), those in the middle values after a single injection (injection group), and those on the right results of the hydrogel application (gel group). Significant differences in BDNF concentrations in the perilymph were detected between the control and gel groups and the injection and gel groups. *Multiple comparisons with the Tukey–Kramer test. Bars represent SDs.

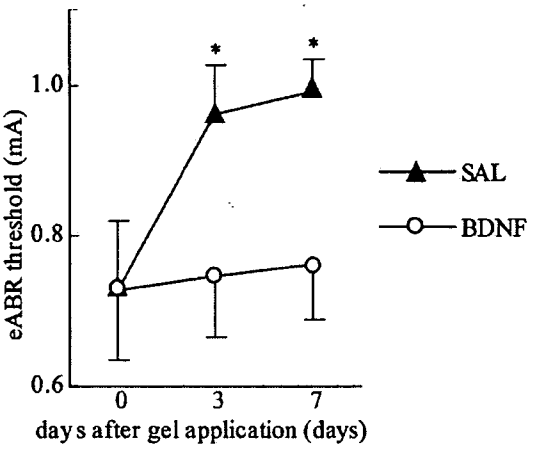

Fig. 2. Functional assessment of the protective effects of brain-derived neurotrophic factor (BDNF) applied by way of a hydrogel against the consecutive degeneration of spiral ganglion neurons (SGN) after hair cell loss. Evoked auditory brain-stem response (eABR) thresholds 0, 3, and 7 days after BDNF application (BDNF) by way of the hydrogel (open circles). eABR thresholds 0, 3, or 7 days after physiologic saline application by way of the hydrogel (control group [SAL]) (closed triangles). Significant differences in the eABR thresholds were detected between the BDNF and SAL groups 3 or 7 days after application. *Multiple comparisons with the Tukey–Kramer test. Bars represent SDs.

Histologic Protection

Immunohistochemistry for NF confirmed the lack of degeneration of SGNs in the cochleae before drug application: the densities (cells/10,000 μm^2) were 25.66 ± 3.26 for the basal turn, 23.77 ± 4.37 for the second turn, and 19.64 ± 3.02 for the third turn. The densities of type II SGNs before drug application were 0.76 ± 0.31 for the basal turn, 0.65 ± 0.52 for the second turn, and 0.71 ± 0.47 for the third turn. Severe degeneration of the SGNs was observed in the SAL group (Fig. 3, D, E, and F) and was apparent in the basal portion of the cochleae: the densities were 3.46 ± 0.88 for the basal turn, 6.52 ± 2.95 for the second turn, and 7.19 ± 3.47 for the third turn. By contrast, no significant degeneration of type II SGNs was observed in the cochleae of the SAL group (Fig. 3, D, E, and F): the densities were 0.73 ± 0.68 for the basal turn, 0.53 ± 0.77 for the second turn, and 0.99 ± 0.38 for the third turn. Although degeneration of the SGNs was detected in the BDNF group, it was limited in comparison with that observed in the SAL group (Fig. 3, A, B, and C):

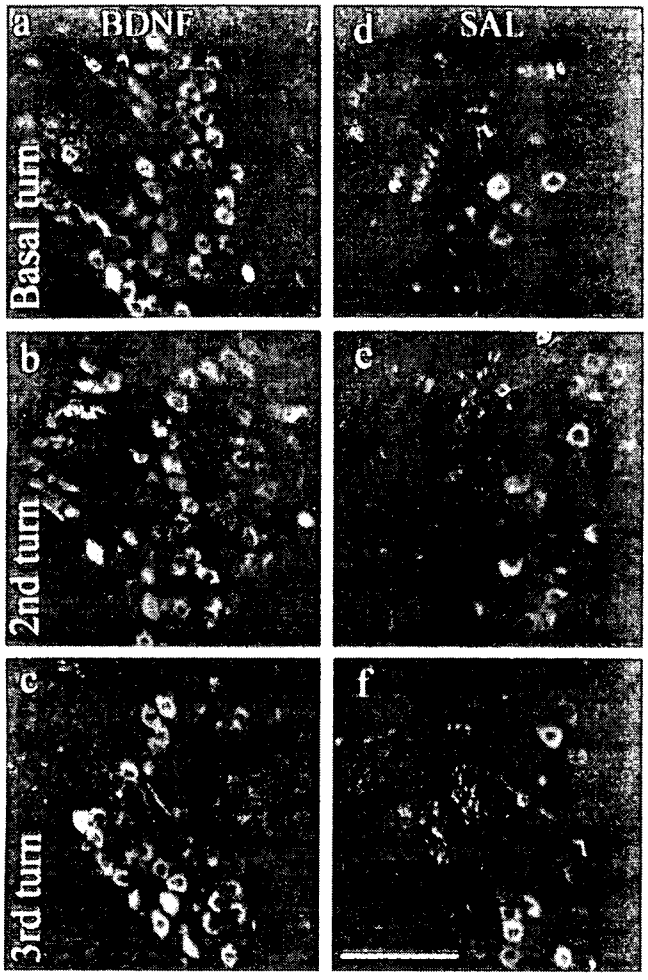

Fig. 3. Immunohistologic evaluation of degeneration of the spiral ganglion neurons (SGN) in each turn of the cochleae 7 days after treatment with a hydrogel immersed with brain-derived neurotrophic factor (BDNF) solution or physiologic saline alone. Immunohistochemistry for neurofilament 200 kD reveals neurons in the Rosenthal's canal (red), whereas immunohistochemistry for peripherin labels type II SGNs (green). Images of SGNs treated with BDNF solutions (BDNF; A to C). SGNs treated with physiologic saline alone (SAL; D to F). Degeneration of the SGNs is apparent in the SAL specimens compared with the BDNF specimens, whereas no significant differences are visible in type II SGNs. Scale bar = 50 μm.

the densities were 11.35 ± 2.77 for the basal turn, 17.97 ± 4.69 for the second turn, and 26.61 ± 8.44 for the third turn. The differences in SGN densities between the BDNF and SAL groups were significant for each turn of the cochleae ($P < .001$) (Fig. 4). No apparent degeneration of the type II SGNs was observed in the BDNF group: the densities were 0.77 ± 0.92 for the basal turn, 0.89 ± 0.93 for the second turn, and 1.09 ± 0.98 for the third turn. No significant differences were observed between the two experimental groups in the densities of type II SGNs in each turn of the cochleae. These findings indicate that type I SGNs are predominantly degenerated in this model and that BDNF application by way of the hydrogel promotes their survival.

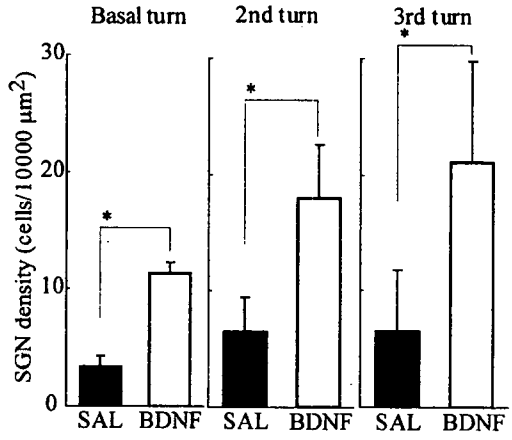

Fig. 4. Densities of spiral ganglion neurons (SGN) in each turn of the cochleae treated with brain-derived neurotrophic factor (BDNF) solution or physiologic saline. Densities of SGNs in cochleae administered BDNF solution after ototoxic treatment (BDNF; bars on right). Densities of SGNs in cochleae administered physiologic saline after ototoxic treatment (SAL; bars on left). *$P < .001$; unpaired t test. Bars represent SDs.

DISCUSSION

Our findings demonstrate the efficient transfer of BDNF into the inner ear using a biodegradable hydrogel. This indicates that the placement of a biodegradable hydrogel on the RWM is an effective method for the local application of neurotrophins to the inner ear. ELISA analyses in the present study confirmed the sustained delivery of BDNF to the cochlear fluid for 7 days by way of the biodegradable hydrogel. In addition, the functional and morphologic protection of SGNs was observed 7 days after BDNF application, indicating that its biological effects were maintained during this period. Biodegradable hydrogels can be injected through the tympanic membrane, and this relatively straightforward procedure can be performed at outpatient clinics by general otolaryngologists.

Previous studies investigating the efficacy of neurotrophins against inner ear degeneration have used the implantation of an osmotic minipump[9,14] or gene transfer by virus vectors[10,15] as drug-application methods. The osmotic minipump is implanted into the subcutaneous tissue, and a tube from the pump is inserted into the basal turn of the cochlea. This method can provide the stable transfer of neurotrophins into the cochlear fluid, resulting in the successful protection of SGNs.[9,14] The use of osmotic minipumps requires middle and inner ear surgery, whereas that of hydrogels only involves positioning the hydrogel on the RWM. Gene transfer using adeno or adeno-associated vectors is an established method for introducing genes of neurotrphins into the inner ear.[10,15] Although recent studies using virus vectors have shown no significant toxicity, this risk remains a major problem in clinical applications. In contrast with virus vectors, biodegradable hydrogels are made from porcine collagen and have no toxity.[6–8] We, therefore, consider the biodegradable hydrogel to be better suited for clinical use than the osmotic minipump or gene transfer.

CONCLUSION

Efforts to reduce degeneration in the inner ear have identified several agents for the protection of hair cells or SGNs. Among these are trophic factors, several of which are commercially available for clinical use. Previous experimental studies have confirmed the protective effects of trophic factors for the inner ear. In the current study, we chose to apply BDNF because its protective effect on SGNs has been verified in several studies using diverse methods. However, biodegradable hydrogels could be used for the delivery of a number of other trophic factors. We believe that our findings will help to advance the clinical application of trophic factors for the treatment of inner ear diseases.

Acknowledgments

The authors thank Norio Yamamoto for generously supporting us with ELISA, Rika Sadato for technical assistant of histologic analysis, and Toshihiro Kushibiki for making the hydrogel.

BIBLIOGRAPHY

1. Nordmann AS, Bohne BA, Harding GW. Histopathological differences between temporaryand permanent threshold shift. *Hear Res* 2000;139:13–30.
2. Nadol JJ, Young YS, Glynn RJ. Survival of spiral ganglion cells in profound sensorineural hearing loss: implications for cochlear implantation. *Ann Otol Rhinol Laryngol* 1989; 98:411–416.
3. Juhn SK, Rybak LP. Labyrinthine barriers and cochlear homeostasis. *Acta Otolaryngol* 1981;91:529–534.
4. Lefebvre PP, Staecker H. Steroid perfusion of the inner ear for sudden sensorineural hearing loss after failure of conventional therapy: a pilot study. *Acta Otolaryngol* 2002; 122:698–702.
5. Minor LB, Schessel DA, Carey JP. Meniere's disease. *Curr Opin Neurol* 2004;17:9–16.
6. Tabata Y, Ikada Y. Controlled release of vascular endothelial growth factor by use of collagen hydrogels. *J Biomater Sci Polym Ed* 2000;11:915–930.
7. Iwakura A, Fujita M, Kataoka K, et al.Intramyocardial sustained delivery of basic fibroblast growth factor improves angiogenesis and ventricular function in a rat infarct model. *Heart Vessels* 2003;18:93–99.
8. Yamamoto M, Takahashi Y, Tabata Y. Controlled release by biodegradable hydrogels enhances the ectopic bone formation of bone morphogenetic protein. *Biomaterials* 2003;24: 4375–4383.
9. Shinohara T, Bredberg G, Ulfendahl M, et al.Neurotrophic factor intervention restores auditory function in deafened animals. *Proc Natl Acad Sci U S A* 2002;99:1657–1660.
10. Nakaizumi T, Kawamoto K, Minoda R, et al. Adenovirus-mediated expression of brain-derived neurotrophic factor protects SGNs from ototoxic damage. *Neurootology* 2004;9: 135–143.
11. West BA, Brummett RE, Himes DL. Interaction of kanamycin and ethacrynic acid. Severe cochlear damage in guinea pigs. *Arch Otolaryngol* 1973;98:32–37.
12. Hall RD. Estimation of surviving spiral ganglion cells in the deaf rat using the electrically evoked auditory brainstem response. *Hear Res* 1990;49:155–168.
13. Mou K, Hunsberger CL, Cleary JM, et al. Synergistic effects of BDNF and NT-3 on postnatal spiral ganglion neurons. *J Comp Neurol* 1997;386:529–539.
14. Ylikoski J, Pirvola U, Suvanto J, et al. Guinea pig auditory neurons are protected by glial cell line-derived neurotrophic factor from degeneration after noise trauma. *Hear Res* 1998;124:17–26.
15. Yagi M, Magal E, Sheng Z, et al .Hair cell protection from aminoglycoside ototoxicity by adenovirus-mediated overexpression of glial cell line-derived neurotrophic factor. *Hum Gene Ther* 1999;10:813–823.

ARTICLE

doi:10.1016/j.ymthe.2006.06.012

Cell–Gene Delivery of Brain-Derived Neurotrophic Factor to the Mouse Inner Ear

Takayuki Okano, Takayuki Nakagawa,* Tomoko Kita, Tsuyoshi Endo, and Juichi Ito

Department of Otolaryngology–Head and Neck Surgery, Graduate School of Medicine, Kyoto University, 606-8507 Kyoto, Japan

**To whom correspondence and reprint requests should be addressed at the Department of Otolaryngology–Head and Neck Surgery, Graduate School of Medicine, Kyoto University, Kawaharacho 54, Shogoin, Sakyo-ku, 606-8507 Kyoto, Japan. Fax: +81 75 751 7225. E-mail: tnakagawa@ent.kuhp.kyoto-u.ac.jp.*

Available online 7 September 2006

Sensorineural hearing loss is a common disability, but treatment options are currently limited to cochlear implants and hearing aids. Studies are therefore being conducted to provide alternative means of biological therapy, including gene therapy. Safe and effective methods of gene delivery to the cochlea need to be developed to facilitate the clinical application of these therapeutic treatments for hearing loss. In this study, we examined the potential of cell–gene therapy with nonviral vectors for delivery of therapeutic molecules into the cochlea. NIH3T3 cells were transfected with the brain-derived neurotrophic factor (*Bdnf*) gene using lipofection and then transplanted into the mouse inner ear. Immunohistochemistry and Western blotting demonstrated the survival of grafted cells in the cochlea for up to 4 weeks after transplantation. No significant hearing loss was induced by the transplantation procedure. A Bdnf-specific enzyme-linked immunosorbent assay revealed a significant increase in Bdnf production in the inner ear following transplantation of engineered cells. These findings indicate that cell–gene delivery with nonviral vectors may be applicable for the local, sustained delivery of therapeutic molecules into the cochlea.

Key Words: gene therapy, cell transplantation, hearing loss, cochlea, brain-derived neurotrophic factor, nonviral vector

INTRODUCTION

Sensorineural hearing loss (SNHL) is one of the most common disabilities in industrialized countries. Defects in the auditory hair cells, and in their associated spiral ganglion neurons (SGNs), can lead to hearing loss or deafness. Approximately 50% of SNHL cases have a genetic basis, a significant proportion of which is non-syndromic and usually inherited in an autosomal recessive manner [1]. In the past decade, many genetic mutations that cause deafness have been identified, which may contribute to the biological sources available for therapeutic approaches. Should the restoration of mutated genes in the cochlea by gene manipulation become a reality, gene therapy might be a promising method for treating SNHL of genetic origin.

Protecting auditory hair cells and SGNs from irreversible degeneration is a primary objective as inner ear cells have limited regeneration capacity. With the recent increase in understanding of the role of neurotrophic factors, including brain-derived neurotrophic factor (BDNF), on the maintenance of the mature peripheral auditory systems, there have been numerous attempts to define ways to reduce hair cell and SGN degeneration [2–6]. Since neurotrophins have a short serum half-life of just minutes or hours [7], their sustained local delivery is essential for cochlear protection. Previous studies have used viral vectors, particularly adenoviruses or adeno-associated viruses, to deliver neurotrophins to the cochleae [8–13]. However, despite their high transduction efficiency, high titer, and ease of production, viral vectors involve potential toxicity.

Gene therapy could enable the long-term delivery of several agents into the inner ear. Cell transplantation has been used as a means of delivering peptides or proteins into the central nervous system, demonstrating its use as a delivery vehicle for therapeutic molecules [14–16]. In addition, recent studies have demonstrated successful cell transplantation into the mouse cochlea [17,18]. Therefore, transplantation of cells that have been genetically manipulated *in vitro* using nonviral vectors potentially resolves the problem of viral vector toxicity in cochlear gene therapy.

In this study, we conducted an examination of the efficiency of cell–gene delivery into the cochlea for application of therapeutic molecules to the treatment of SNHL. We chose NIH3T3 cells as a delivery vehicle for the

1525-0016/$30.00

gene. NIH3T3 cells are a well-established fibroblast cell line, so that it is easy to optimize conditions for gene transfer and to select gene-expressing cells *in vitro*. In addition, fibroblasts are available from various human sources, which may be advantage for extending future clinical investigations. We transfected NIH3T3 cells with the *Bdnf* gene using lipofection. We then examined the potential for transplanting transfected NIH3T3 cells into the mouse inner ear.

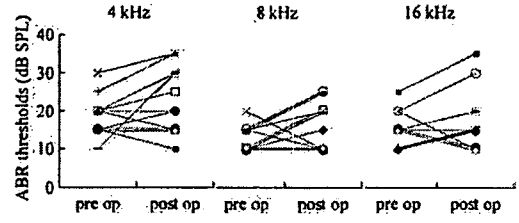

FIG. 1. ABR thresholds before and after cell transplantation. The left lane shows preoperative (pre op) ABR thresholds of each ear, and the right shows those recorded on day 28 after transplantation (post op) at 4, 8, and 16 kHz. The *x* axis shows ABR thresholds (dB SPL).

Results and Discussion

Bdnf Gene Transfer

To determine the efficacy of gene transfection using a nonviral vector, we performed reverse transcriptase-polymerase chain reaction (RT-PCR) analysis of Bdnf mRNA levels in transfected and nontransfected NIH3T3 cells (data not shown). NIH3T3 cells transfected with the mouse *Bdnf* gene (NIH3T3/BDNF) demonstrated Bdnf mRNA expression (86-bp fragment), which was absent from cells transfected with a vector carrying an antibiotic resistance gene (NIH3T3/control) and from nontransfected cells (NIH3T3/original). Amplification of gylceraldehyde-3-phosphate dehydrogenase (*Gapdh*), yielding a 171-bp amplicon, was used as an internal control. Negative control reactions that lacked reverse transcriptase failed to yield amplicons of either *Gapdh* or *Bdnf*.

We carried out an enzyme-linked immunosorbent assay (ELISA) for Bdnf protein to examine the efficacy of Bdnf protein expression and secretion *in vitro*. The mean Bdnf concentration in the culture medium of NIH3T3/BDNF cells, at 396.70 ± 32.66 pg/ml, was significantly higher than in the medium of either NIH3T3/control cells (24.96 ± 5.22 pg/ml) or NIH3T3/original cells (32.42 ± 7.09 pg/ml) ($P < 0.0001$). These findings demonstrate efficient, functional gene transfer into NIH3T3 cells *in vitro* by a liposome-mediated delivery method.

Cell Transplantation into Mouse Cochleae

We transfected NIH3T3 cells with the mouse *Bdnf* gene tagged with a FLAG epitope (NIH3T3/FLAG) to enable transfected, transplanted cells to be readily distinguished from host inner ear cells. We injected suspensions of NIH3T3/FLAG and NIH3T3/control cells into the perilymphatic space of the posterior semicircular canal of C57BL/6 mice using a technique that we developed in previous studies [17,18]. Although delivery of cells into the mouse cochlea is difficult because of its small size, the well-defined genetics of a mouse model enable a variety of analyses of the inner ear to be performed.

We performed auditory brain stem response (ABR) recording to evaluate the effects of the transplantation procedure on hearing (Fig. 1). Alterations in ABR thresholds between pre- and postoperation were limited within 10 dB, although one animal exhibited a 20-dB elevation in ABR thresholds at 4 kHz. Preoperative ABR thresholds were 18.6 ± 1.7 (dB SPL) at 4 kHz, 12.7 ± 1.0 at 8 kHz, and 15.5 ± 1.4 at 16 kHz, and those on postoperative day 28 were 22.7 ± 2.6 at 4 kHz, 15.9 ± 1.9 at 8 kHz, and 17.3 ± 2.5 at 16 kHz. We identified no significant elevation of ABR thresholds on day 28 at frequencies of 4, 8, and 16 kHz. In addition, we observed no vestibular dysfunction in the behavior of the animals after the operation. These findings indicate the limited surgical invasiveness of our transplantation procedure, which is almost identical to previous observations [19,20].

Immunohistochemical analysis of FLAG expression demonstrated the settlement and survival of grafted NIH3T3/FLAG cells in both the cochlea and the vestibule (Figs. 2A, 2B, 2D, 2E). The engrafted cells were clearly distinct from the endogenous cells based on their expression of FLAG, while control specimens that were transplanted with NIH3T3/control cells exhibited no expression of FLAG (Figs. 2C and 2F). Grafted cells were localized in the perilymphatic space of cochleae or vestibules and did not establish in the endolymphatic space or within the inner ear tissues. These locations are identical to those of neural stem cell-derived cells transplanted into the mouse inner ear through the semicircular canal in our previous study [17]. On day 7, we found numerous grafted cells as cell aggregates in the vestibule. On day 28, we still observed grafted cells in both vestibules and cochleae, but did not see aggregation of grafted cells. Of grafted cells located in the perilymphatic space of cochleae, 91.2 ± 11.1% adhered to host cochlear tissues on day 7 and 92.3 ± 14.7% on day 28. The survival and settlement of grafted cells in the inner ear were also demonstrated by Western blotting for FLAG (Fig. 2G). We prepared protein lysates from the inner ear specimens obtained on day 28. The FLAG-tagged *Bdnf* transgene product (31 kDa) was detected in specimens transplanted with NIH3T3/FLAG cells, but not in those transplanted with NIH3T3/control cells. The β-actin internal control was detected in both specimens at equal density. These findings demonstrate that cells transplanted through the posterior semicircular canal survive and produce gene-encoded proteins in the perilymphatic space of cochleae and vestibules, indicating

doi:10.1016/j.ymthe.2006.06.012

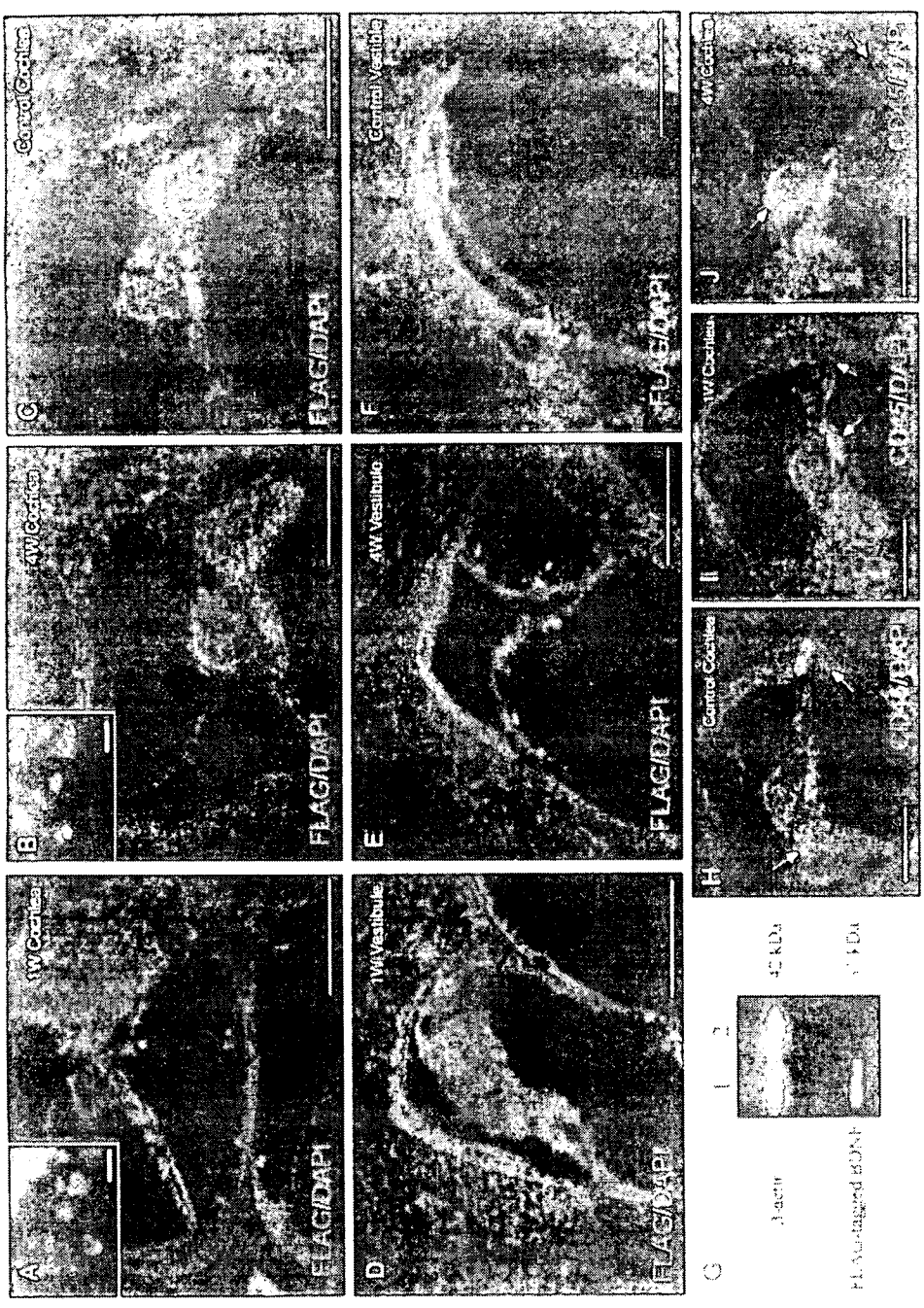

FIG. 2. Localization of grafted NIH3T3/FLAG cells in the inner ear and infiltration of CD45-positive cells in cochleae. (A–F) Grafted cells are labeled with FLAG (green fluorescence), and cell nuclei are labeled with DAPI (blue fluorescence). A number of grafted cells are found both in the cochlea (A) and in the vestibule (D) at 1 week after transplantation. In the vestibule, numerous grafted cells form cell aggregates (D). Grafted cells are also identified in the cochlea (B) and vestibule (E) at 4 weeks after transplantation. No FLAG-positive cells were found in the control cochlea (C) or vestibule (F). Bars represent 200 μm and 20 μm in insets. (G) Western blot for FLAG expression in the inner ear at 4 weeks after cell transplantation. The FLAG-tagged Bdnf (31-kDa band) is detected in cochleae engrafted with NIH3T3/BDNF-FLAG cells (lane 1), but not in engrafted control cells (lane 2). β-Actin (42-kDa band), an internal control, is detected in both specimens at the same density. (H–J) Localization of CD45-positive cells in cochleae. In control cochleae, CD45-positive cells (red fluorescence) are found in the spiral ligament and spiral ganglion (arrows in H). CD45-positive cells were localized in the spiral ganglion, osseous spiral lamina, spiral ligament, and spiral limbus (arrows) at 1 (I) and 4 weeks (J) after engraftment of NIH3T3/BDNF-FLAG cells. Blue fluorescence shows DAPI. Bars represent 200 μm.

sustained delivery of Bdnf from transplanted cells to the perilymphatic space of the inner ears. Previous investigations have demonstrated that application of neurotrophins, including Bdnf, into the perilymph efficiently protects hair cells or spiral ganglion neurons from various ototoxic insults [2–6,10,11], indicating that neurotrophins delivered in the perilymph act on hair cells and spiral ganglion neurons. We therefore consider that Bdnf secreted from transplanted cells may be accessible to hair cells and spiral ganglion neurons.

The numbers of FLAG-positive cells in the cochlea decreased from the time point of day 7 to that of day 28. On day 7 after transplantation, we observed 26.7 ± 3.3 grafted cells in one midmodiolus section of cochleae, while we found 14.4 ± 2.3 cells on day 28. We then analyzed infiltration of inflammatory cells into cochlear tissues to investigate immune-mediated clearance of grafted cells. We employed immunohistochemistry for CD45, a leukocyte common antigen, to determine the distribution of inflammatory cells in the cochlea. In control cochleae, we found CD45-positive cells in the spiral ganglion, spiral limbus, and spiral ligament (Fig. 2H). Cochleae that received transplantation of NIH3T3/FLAG cells exhibited a similar distribution of CD45-positive cells compared to that of control cochleae (Figs. 2I and 2J). We observed no obvious infiltration of CD45-positive cells into the perilymphatic space of cochleae. These findings demonstrate that infiltration of inflammatory cells is not induced by transplantation of NIH3T3/FLAG cells into the inner ears. Even after xenografts into the cochlear fluid space without use of immune suppressants, cell infiltration into the cochlear fluid space has not been observed [21]. We therefore consider that immune-mediated clearance may not play a central role in elimination of transplanted cells from the inner ear. However, further studies are required to determine actual roles of the immune system in the decrease in transplanted cells in the inner ears.

Efficiency of Gene Delivery

We performed an ELISA of Bdnf proteins extracted from the inner ear to examine the efficiency of cell–gene delivery. We collected the inner ear specimens on day 7 after transplantation and calculated the ratio of Bdnf concentration to total protein in the sample solutions. NIH3T3/BDNF cell-transplanted specimens showed a significantly higher ratio (93.40 ± 10.69 pg/mg total protein) compared with NIH3T3/control cell-transplanted samples (46.68 ± 4.41 pg/mg) ($P = 0.01$). There was no significant difference between the levels of total protein extracted from the two samples (NIH3T3/BDNF, 2.65 ± 0.21 mg/ml; NIH3T3/control, 2.77 ± 0.12 mg/ml). These findings demonstrate that Bdnf synthesis by engrafted NIH3T3/BDNF cells contributes to a significant increase in Bdnf protein levels of the inner ear specimens, suggesting that cell–gene therapy may be applicable for local, sustained delivery of therapeutic molecules into the inner ear.

This is the first report that demonstrates the successful cell–gene delivery of therapeutic molecules to the cochlea without the use of viral vectors, an encouraging result for the extension of research into gene therapy for the inner ear. Currently, several experiments utilize human fibroblasts as a delivery vehicle [22,23]. The use of autologous bone marrow-derived stromal cells for transplants into the inner ear has been reported [24]. Such cells eliminate the risk of immunoresponses, and their ability to migrate into the cochlear lateral wall and modiolus is likely to enhance the potential for delivery of genes into these areas of the cochlea. Future studies should be performed to evaluate the potential of these alternative transplant media as a vehicle for gene delivery.

In summary, we transplanted NIH3T3 cells that had been genetically engineered to express Bdnf into the mouse inner ear and evaluated the efficiency of transplantation for local delivery of gene products. The results demonstrated a significant increase in Bdnf protein in the inner ear following transplantation of engineered cells. These findings indicate that gene therapy may be a feasible treatment option for inner ear diseases such as SNHL. Cell–gene delivery of therapeutic molecules into the inner ear is suitable for protection of inner ear cells against gradually progressive degeneration. Presbycusis, age-related hearing loss, may be included in targets for cell–gene therapy. BDNF application via cell–gene delivery could be an efficient strategy for promotion of survival of SGNs in cases of cochlear implants (CIs), which are small devices that are surgically implanted in the cochlea to stimulate SGNs. BDNF transgene produced by gene-engineered cells will support the survival of SGNs after CI surgery, which can contribute to the maintenance of hearing benefits provided by CIs.

Materials and Methods

Animals. Forty-three 10-week-old male C57BL/6 mice (SLC Japan, Hamamatsu, Japan) with normal hearing were used in the study. All mice were maintained in the Institute of Laboratory Animals, Kyoto University Graduate School of Medicine. All experimental protocols were approved by the Animal Research Committee, Kyoto University Graduate School of Medicine, and conducted in accordance with NIH guidelines for the care and use of laboratory animals.

Vector construction. The *Mus musculus* (house mouse) brain-derived neurotrophic factor cDNA clone (GenBank Accession No. BC034862) was obtained from Invitrogen (Carlsbad, CA, USA). PCR amplification of the cDNA using Pyrobest DNA polymerase (TaKaRa-Bio, Kyoto, Japan) was performed with the following primer pairs: 5′ primer, 5′-GGAATTCGCCACCATGACCATCCTTTTCCTTACTATGG-3′; 3′ primer 1, 5′-ATAAGAATAAGCGGCCGCTCATCTTCCCCTTTTAATGGTCAGTG-3′; and 3′ primer 2, incorporating two pairs of FLAG epitope, 5′-ATAAGAATAAGCGGCCGCTCACTTGTCATCGTCGTCCTTGTAGTCCTTGTCATCGTCGTCCTTGTAGTCCTTGTCATCGTCGTCCTTGTAGTCTCTTCCCCTTTTAATGGTCAGTG-3′. PCR products were digested with *Eco*RI and *Not*I, and a 0.77-kb

doi:10.1016/j.ymthe.2006.06.012

*Eco*RI–*Not*I fragment containing mouse *Bdnf* or mouse *Bdnf* with FLAG epitope was cloned into the *Eco*RI–*Not*I site of the pIRESneo3 vector (BD Biosciences, Palo Alto, CA, USA) using Ligation Solution (TaKaRa-Bio) to generate plasmid pIRESneo3-bdnf (supplementary information) or pIRESneo3-bdnfflag. For subsequent experiments, plasmid pIRESneo3 containing the neomycin-resistant gene only (pIRESneo3-control) was also amplified. Restriction analysis and DNA sequencing were used to confirm the integrity of all constructs.

Cell lines and gene transfer. NIH3T3 cells were obtained from Riken Cell Bank (RCB 0150; Tsukuba, Japan) and cultured in Dulbecco's modified Eagle's medium (DMEM; GIBCO BRL, Grand Island, NY, USA) containing 10% newborn calf serum (GIBCO), penicillin (100 U/ml), streptomycin (100 μg/ml), and amphotericin B (0.25 μg/ml) in a humidified atmosphere of 5% CO_2 at 37°C. NIH3T3 cells were plated at a density of 1×10^5 cells per 100-mm plastic dish and incubated for 48 h. Transfection was performed with 18 μl of FuGENE6 Transfection Reagent (Roche, Indianapolis, IN, USA) complexed with 9 μg pIRESneo3-bdnf, pIRESneo3-bdnfflag, or pIRESneo3-control plasmid in DMEM per 100-mm plastic dish at 37°C for 6 h. The medium was then replaced with conditioned medium containing Geneticin sulfate (G418; Sigma, St. Louis, MO, USA) for the selection of stably transfected cell clones.

Bdnf mRNA expression in cell lines. The expression of Bdnf mRNA in the cell lines was analyzed with RT-PCR. Total RNA was extracted from the cultured cell lines using the RNeasy Kit (Qiagen GmbH, Germany) and then treated with DNase I (Ambion, Austin, TX, USA). Four sets of total RNA for each cell line were prepared. PCRs were performed using TaqMan Gold PCR Master Mix (Applied Biosystems, Foster City, CA, USA) and Bdnf-specific primers. Gapdh mRNA was used as the invariant control. All reactions were performed in triplicate.

Bdnf secretion from cell lines. Bdnf protein levels in culture medium were measured by ELISA to examine Bdnf secretion by transfected cells. NIH3T3/BDNF, NIH3T3/control, and NIH3T3/original cells (1×10^5) were inoculated in 60-mm plastic dishes with 3 ml conditioned medium. The supernatants of the conditioned media were harvested approximately 24 h after inoculation. ELISA was performed using the BDNF Emax Immunoassay System (Promega, Madison, WI, USA) according to the manufacturer's instructions. Four sets of samples were prepared from each cell line, and all reactions were performed in triplicate.

Cell transplantation. On the day of transplantation, cultured cells were suspended at 3×10^4 cells/μl DMEM/F12 (GIBCO). NIH3T3/BDNF cells were transplanted into 10 animals, NIH3T3/FLAG cells into 24 animals, and NIH3T3/control cells into 9 animals. Cell transplantation was performed under general anesthesia with 75 mg/kg ketamine and 9 mg/kg xylazine. A retroauricular incision was made in the left ear, and the posterior semicircular canal (PSCC) was exposed. A small hole was made in the bony wall of the PSCC. A fused silica glass needle (EiCOM, Kyoto, Japan) was then inserted into the perilymphatic space of the PSCC, and the cell suspension was injected at the rate of 1 μl/min for 3 min using a Micro Syringe Pump (EiCOM).

Measurement of auditory function. The auditory function of experimental animals was monitored by ABR recording. ABR measurements were performed as previously described [25]. ABRs were recorded before cell transplantation and on day 28 in the 11 animals that received an engraftment of NIH3T3/FLAG cells. Thresholds were determined for frequencies of 4, 8, and 16 kHz.

Immunohistochemistry. Under general anesthesia, the animals that had been engrafted with NIH3T3/BDNF-FLAG cells were transcardially perfused with phosphate-buffered saline, pH 7.4, followed by 4% paraformaldehyde in phosphate buffer at pH 7.4 on day 7 ($n=10$) or 28 ($n=10$). Immediately, the temporal bones were dissected out and immersed in the same fixative for 4 h at 4°C. Specimens were prepared as cryostat sections. Two midmodiolus sections were chosen from each specimen and stained by immunohistochemistry for FLAG to distinguish transplanted cells from host specimens. Two cochleae on day 7 after transplantation of NIH3T3/control cells were used as controls for immunostaining for FLAG. We counted the numbers of FLAG-positive cells and those of FLAG-positive cells that adhered to cochlear tissues. The ratios of grafted cell that adhered to cochlear tissues were then calculated. The emergence of CD45-positive cells was also examined to evaluate inflammatory response following cell transplantation. Untreated cochlear specimens were served as controls for immunostaining for CD45. Anti-FLAG M2 mouse monoclonal antibody (1:230; Sigma) or anti-mouse CD45 rat monoclonal antibody (a leukocyte common antigen, Ly-5, 1:20; BD PharMingen, San Diego, CA, USA) was used as the primary antibody, and FITC-conjugated goat anti-mouse antibody (1:500; Santa Cruz Biotechnology, Santa Cruz, CA, USA) or Alexa-Fluor 546-conjugated anti-rat antibody (1:500; Molecular Probes, Eugene, OR, USA) was used as the secondary antibody. Counterstaining by 4',6-diamidino 2-phenylindole dihydrochloride (DAPI; 1 μg/ml; Molecular Probes) was performed to demonstrate nuclear locations.

FLAG Western blotting. The expression of FLAG-tagged Bdnf fusion protein in the inner ear engrafted with NIH3T3/FLAG cells ($n=4$) or NIH3T3/control cells ($n=4$) was determined by Western blotting 28 days after transplantation. The temporal bones were homogenized in ice-cold lysis buffer. After centrifugation of the homogenized solution, the supernatants were assayed for proteins. The sample solutions were electroblotted onto a polyvinyldifluoride membrane. The primary antibody was a mouse monoclonal anti-FLAG antibody (1:500; Sigma) or rabbit polyclonal anti-β-actin antibody (1:200; Sigma), and the secondary antibody was HRP-conjugated anti-mouse IgG (1:50,000; Amersham Biopharmacia Biotech, Buckinghamshire, UK) or anti-rabbit IgG (1:25,000; Amersham Biopharmacia Biotech). Reactions were visualized by chemiluminescence using an ECL Plus Western blotting reagent pack (Amersham Biopharmacia Biotech).

Measurement of Bdnf levels in the inner ear. To assess the *in vivo* production of Bdnf protein by grafted cells, the inner ears engrafted with NIH3T3/BDNF cells ($n=10$) or NIH3T3/control cells ($n=5$) were removed on day 7 after transplantation. A Bdnf ELISA was performed using the BDNF Emax Immunoassay System (Promega) according to the manufacturer's protocol. All reactions were performed in triplicate. Total protein concentration was measured with the Lowry assay using the Bio-Rad DC Protein Assay (Bio-Rad, Hercules, CA, USA).

Statistical analysis. Results were expressed as means ± standard error. Statistical analyses for Bdnf levels in the cultured medium and ABR threshold shifts were performed using one-way ANOVA followed by Sheffe's multiple-comparison tests. A Mann–Whitney *U* test was used to compare cochlear Bdnf levels. Probability (*P*) values less than 5% were considered significant.

ACKNOWLEDGMENTS

The authors thank Daisuke Yabe and Norio Yamamoto (Department of Medical Chemistry and Molecular Biology, Kyoto University Graduate School of Medicine, Japan) for help and instruction with molecular biology, Junko Okano (Department of Anatomy and Developmental Biology, Kyoto University Graduate School of Medicine) for critical discussion, and Yoko Nishiyama and Rika Sadato for their technical assistance. This study was supported by a Grant-in-Aid for Scientific Research (B2, 16390488, 2004–2006, T.N.) from the Ministry of Education, Culture, Sports, Science, and Technology of Japan and in part by a grant (2005–2006, T.N.) from the Takeda Science Foundation and a grant (2005, T.O.) from the 21st Century COE Program of the Ministry of Education, Culture, Sports, Science, and Technology of Japan.

RECEIVED FOR PUBLICATION MARCH 7, 2006; REVISED JUNE 8, 2006; ACCEPTED JUNE 21, 2006.

APPENDIX A. SUPPLEMENTARY DATA

Supplementary data associated with this article can be found, in the online version, at doi:10.1016/j.ymthe.2006.06.012.

REFERENCES

1. Nance, W. E. (2003). The genetics of deafness. *Ment. Retard. Dev. Disabil. Res. Rev.* **9:** 109–119.
2. Altschuler, R. A., Cho, Y., Ylikoski, J., Pirvola, U., Magal, E., and Miller, J. M. (1999). Rescue and regrowth of sensory nerves following deafferentation by neurotrophic factors. *Ann. N.Y. Acad. Sci.* **884:** 305–311.
3. Gillespie, L. N., Clark, G. M., Bartlett, P. F., and Marzella, P. L. (2003). BDNF-induced survival of auditory neurons in vivo: cessation of treatment leads to accelerated loss of survival effects. *J. Neurosci. Res.* **71:** 785–790.
4. Endo, T., *et al.* (2005). Novel strategy for treatment of inner ears using a biodegradable gel. *Laryngoscope* **115:** 2016–2020.
5. Noushi, F., Richardson, R. T., Hardman, J., Clark, G., and O'Leary, S. (2005). Delivery of neurotrophin-3 to the cochlea using alginate beads. *Otol. Neurotol.* **26:** 528–533.
6. Shinohara, T., *et al.* (2002). Neurotrophic factor intervention restores auditory function in deafened animals. *Proc. Natl. Acad. Sci. USA* **99:** 1657–1660.
7. Kishino, A., *et al.* (2001). Analysis of effects and pharmacokinetics of subcutaneously administered BDNF. *Neuroreport* **12:** 1067–1072.
8. Staecker, H., Gabaizadeh, R., Federoff, H., and Van De Water, T. R. (1998). Brain-derived neurotrophic factor gene therapy prevents spiral ganglion degeneration after hair cell loss. *Otolaryngol. Head Neck Surg.* **119:** 7–13.
9. Chen, X., Frisina, R. D., Bowers, W. J., Frisina, D. R., and Federoff, H. J. (2001). HSV amplicon-mediated neurotrophin-3 expression protects murine spiral ganglion neurons from cisplatin-induced damage. *Mol. Ther.* **3:** 958–963.
10. Yagi, M., Magal, E., Sheng, Z., Ang, K. A., and Raphael, Y. (1999). Hair cell protection from aminoglycoside ototoxicity by adenovirus-mediated overexpression of glial cell line-derived neurotrophic factor. *Hum. Gene Ther.* **10:** 813–823.
11. Hakuba, N., *et al.* (2003). Adenovirus-mediated overexpression of a gene prevents hearing loss and progressive inner hair cell loss after transient cochlear ischemia in gerbils. *Gene Ther.* **10:** 426–433.
12. Nakaizumi, T., Kawamoto, K., Minoda, R., and Raphael, Y. (2004). Adenovirus-mediated expression of brain-derived neurotrophic factor protects spiral ganglion neurons from ototoxic damage. *Audiol. Neurootol.* **9:** 135–143.
13. Stone, I. M., Lurie, D. I., Kelley, M. W., and Poulsen, D. J. (2005). Adeno-associated virus-mediated gene transfer to hair cells and support cells of the murine cochlea. *Mol. Ther.* **11:** 843–848.
14. Cejas, P. J., *et al.* (2000). Lumbar transplant of neurons genetically modified to secrete brain-derived neurotrophic factor attenuates allodynia and hyperalgesia after sciatic nerve constriction. *Pain* **86:** 195–210.
15. Cao, L., *et al.* (2004). Olfactory ensheathing cells genetically modified to secrete GDNF to promote spinal cord repair. *Brain* **127:** 535–549.
16. Girard, C., *et al.* (2005). Grafts of brain-derived neurotrophic factor and neurotrophin 3-transduced primate Schwann cells lead to functional recovery of the demyelinated mouse spinal cord. *J. Neurosci.* **25:** 7924–7933.
17. Iguchi, F., *et al.* (2003). Trophic support of mouse inner ear by neural stem cell transplantation. *Neuroreport* **14:** 77–80.
18. Tateya, I., *et al.* (2003). Fate of neural stem cells grafted into injured inner ears of mice. *Neuroreport* **14:** 1677–1681.
19. Iguchi, F., *et al.* (2004). Surgical techniques for cell transplantation into the mouse cochlea. *Acta Otolaryngol. Suppl.* **551:** 43–47.
20. Kawamoto, K., Oh, S. H., Kanzaki, S., Brown, N., and Raphael, Y. (2001). The functional and structural outcome of inner ear gene transfer via the vestibular and cochlear fluids in mice. *Mol. Ther.* **4:** 575–585.
21. Hildebrand, M. S., *et al.* (2005). Survival of partially differentiated mouse embryonic stem cells in the scala media of the guinea pig cochlea. *J. Assoc. Res. Otolaryngol.* **6:** 341–354.
22. Evans, C. H., *et al.* (2005). Gene transfer to human joints: progress toward a gene therapy of arthritis. *Proc. Natl. Acad. Sci. USA* **102:** 8698–8703.
23. Kakeda, M., *et al.* (2005). Human artificial chromosome (HAC) vector provides long-term therapeutic transgene expression in normal human primary fibroblasts. *Gene Ther.* **12:** 852–856.
24. Naito, Y., *et al.* (2004). Transplantation of bone marrow stromal cells into the cochlea of chinchillas. *Neuroreport* **15:** 1–4.
25. Shiga, A., *et al.* (2005). Aging effects on vestibulo-ocular responses in C57B/6 mice: comparison with alteration in auditory function. *Audiol. Neurootol.* **10:** 97–104.

European Journal of Neuroscience, Vol. 25, pp. 2307–2318, 2007 doi:10.1111/j.1460-9568.2007.05478.x

Transplantation of conditionally immortal auditory neuroblasts to the auditory nerve

Tetsuji Sekiya,[1,*] Matthew C. Holley,[3,*] Ken Kojima,[1,2] Masahiro Matsumoto,[1] Richard Helyer[4] and Juichi Ito[1]
[1]Departments of Otolaryngology – Head and Neck Surgery, Kyoto University Graduate School of Medicine, Sakyou-ku, Kyoto, 606–8507 Japan
[2]Establishment of International Center of Excellence (COE) for Integration of Transplantation Therapy and Regenerative Medicine, Kyoto University Graduate School of Medicine; Sakyou-ku, Kyoto, Japan
[3]Department of Biomedical Science, The University of Sheffield, England
[4]Department of Physiology, University of Bristol, England

Keywords: cell line, cell transplantation, hearing loss, immortomouse, *in vivo*, spiral ganglion neuron

Abstract

Cell transplantation is a realistic potential therapy for replacement of auditory sensory neurons and could benefit patients with cochlear implants or acoustic neuropathies. The procedure involves many experimental variables, including the nature and conditioning of donor cells, surgical technique and degree of degeneration in the host tissue. It is essential to control these variables in order to develop cell transplantation techniques effectively. We have characterized a conditionally immortal, mouse cell line suitable for transplantation to the auditory nerve. Structural and physiological markers defined the cells as early auditory neuroblasts that lacked neuronal, voltage-gated sodium or calcium currents and had an undifferentiated morphology. When transplanted into the auditory nerves of rats *in vivo*, the cells migrated peripherally and centrally and aggregated to form coherent, ectopic 'ganglia'. After 7 days they expressed β3-tubulin and adopted a similar morphology to native spiral ganglion neurons. They also developed bipolar projections aligned with the host nerves. There was no evidence for uncontrolled proliferation *in vivo* and cells survived for at least 63 days. If cells were transplanted with the appropriate surgical technique then the auditory brainstem responses were preserved. We have shown that immortal cell lines can potentially be used in the mammalian ear, that it is possible to differentiate significant numbers of cells within the auditory nerve tract and that surgery and cell injection can be achieved with no damage to the cochlea and with minimal degradation of the auditory brainstem response.

Introduction

Sensorineural hearing loss affects 250 million people worldwide and is in most cases associated with a permanent loss of sensory hair cells and their afferent sensory neurons (Holley, 2005). Cell replacement might be achieved by new techniques in gene therapy (Izumikawa *et al.*, 2005) and cell transplantation (Li *et al.*, 2004; Sekiya *et al.*, 2006). Transplantation of auditory sensory neurons could benefit patients with neuropathic hearing loss (Starr *et al.*, 1996) and following treatment for vestibular Schwannoma (Samii & Matthies, 1997; Regis *et al.*, 2002). It could also provide benefits in conjunction with cochlear and brainstem implants, where the preservation of auditory neurons is crucial for a successful outcome and for preservation of function in the higher relay nuclei (Kopke *et al.*, 1996; Altschuler *et al.*, 1999).

Cell transplantation is a complex procedure and hearing research shares similar conflicting issues to those encountered in other fields, notably that of Parkinson's Disease (Lindvall *et al.*, 2004; Winkler *et al.*, 2005). In the first instance, there is a desire to show that the approach will work in principle, which involves demonstrating functional recovery from an *in vivo* experiment as quickly as possible. However, the large number of experimental variables can compromise the outcome and confuse the chances of more structured progress (Winkler *et al.*, 2005). These variables include selection and conditioning of donor cells, the nature of the surgery for cell delivery and the degenerative state of the recipient tissue. Cell transplantation to the auditory system has been attempted with embryonic tissue (Ito *et al.*, 2001; Hu *et al.*, 2004), embryonic stem cells (Okano *et al.*, 2005; Corrales *et al.*, 2006; Sekiya *et al.*, 2006) and tissue-specific stem cells (Iguchi *et al.*, 2003; Hakuba *et al.*, 2005; Hu *et al.*, 2005) that have been conditioned or genetically modified before or after delivery (Hu *et al.*, 2005; Sekiya *et al.*, 2006). The recipient animals have included several different experimental models in mice (Tamura *et al.*, 2004), rats (Sekiya *et al.*, 2000), gerbils (Lang *et al.*, 2005) chinchillas (Naito *et al.*, 2004), guinea pigs (Olivius *et al.*, 2004) and chickens (Sakamoto *et al.*, 2004) with or without damage in addition to the surgical delivery technique. We have attempted to control some of the less predictable variables so that we can go on to explore the influence of host tissue degeneration, preconditioning of cells and simultaneous treatment with extrinsic agents such as growth factors.

In this work we have used a conditionally immortal cell line derived from embryonic mouse auditory neuroblasts (Nicholl *et al.*, 2005), characterized its state of physiological differentiation and explored its behaviour *in vivo*, including its affect on the auditory brainstem responses.

Correspondence: Dr Tetsuji Sekiya, as above.
E-mail: tsekiya@ent.kuhp.kyoto-u.ac.jp

*T.S. and M.C.H. contributed equally to this work.

Received 4 September 2006, revised 28 January 2007, accepted 12 February 2007

Materials and methods

Cell culture

To maintain proliferation the neuroblast cell line US/VOT-N33 (VOT-N33) was cultured in Neurobasal medium (NB) supplemented with 0.5 mM L-glutamine (Invitrogen-Gibco), 2.5% bovine fetal calf serum (FCS) and 50 units/mL γ-interferon (γIF) at 33 °C. For differentiating conditions the γIF was removed to decrease expression of the immortalizing gene and the cells were incubated at 39 °C to render the T-antigen unstable. Prior to experimentation cells were cultured in a 35 mm dish under proliferating conditions in 1 mL NB + 2.5% FCS overnight to promote attachment. The next day the media was replaced with NB + 2% B27 supplement (Invitrogen-Gibco). On the day of transplantation the gamma interferon was removed. Transplanted cells were stably transfected with a constitutively expressed, enhanced green fluorescent protein (EGFP), which allowed them to be identified *in vivo*. Transfections were performed using Fugene 6 transfection reagent (Roche, East Sussex, UK) following the manufacturer's protocols. The construct contained a CAG enhancer (a combination of chicken β-actin promoter and cytomegalovirus immediate-early enhancer) driving expression of a bicistronic message encoding EGFP and resistance to puromycin. Initial selection of transfected cells was performed using 10 μg/mL puromycin, while selective pressure was maintained at 2.5 μg/mL for cells routinely cultured with γIF at 33 °C.

Cell electrophysiology

Cells were allowed to grow under differentiating conditions for a minimum of 6 days before recording. We were able to culture them for over 30 days, during which time the medium was replaced every 5 days. Prior to electrophysiology, the culture medium was removed and cells washed with extracellular solution (ECS, see below). Cells were removed by application of Hanks solution (Sigma) with added HEPES buffer (Gibco) at 0.5% and containing 10× trypsin solution (Sigma) at 10%. After the cells had detached the trypsin was immediately neutralized by 1× trypsin inhibitor (Sigma) in Hanks solution. The cells were then spun for 2 min at 600 ***g***, the supernatant aspirated, and the cells gently resuspended in 1 mL ECS. The suspension was placed in a recording chamber and the cells allowed to settle to the chamber base prior to recording. Experiments were typically of 1 h duration.

Whole-cell patch-clamp was used to record membrane currents of single cells at room temperature (20–25 °C). The extracellular solution contained (in mM) 135 NaCl, 0.7 NaH_2PO_4, 5.8 KCl, 1.3 $CaCl_2$, 0.9 $MgCl_2$, 5.6 D-glucose, 10 HEPES-NaOH. Amino acids and vitamins for Eagle's MEM were added from concentrates (Life Technologies). The pH was adjusted to 7.4, and the osmolality was ~304 mOsm/kg. The concentration of NaCl was altered to maintain the osmolality in solutions containing caesium (Cs^+), barium (Ba^{2+}) and cadmium (Cd^{2+}). Patch pipettes were pulled from soda-glass capillaries (Clark Electromedical Instruments). To reduce the electrode capacitance the shank of the electrode was coated with wax. The pipette filling solution contained (in mM) 145 KCl, 3 $MgCl_2$, 5 Na_2ATP, 1 EGTA-KOH, 5 HEPES-KOH, pH 7.3 (288 mOsm/kg). Recording electrodes had resistances in the bath of typically between 2.4 and 3.2 MΩ. During recording the cells were perfused at a rate of approximately 0.5 mL/min with ECS. Solutions containing other ions were added by whole bath perfusion.

A Cairn Optopatch patch-clamp amplifier was used for recordings, connected to an Axon Instruments Digidata 1200B interface (Axon Instruments, Foster City, CA). Data acquisition was performed using Axon Instruments pClamp software. Data were filtered at 3 kHz, sampled at 5 kHz, and stored on computer for off-line analysis. Residual series resistance after compensation (0–60%) was typically in the range 2–10 MΩ. Recordings and reported currents were corrected off-line for linear leakage and in some cases for residual capacitative transients. Membrane potentials were corrected for errors due to series resistance, and for a liquid junction potential of 4 mV calculated between pipette and bath solutions.

RT-PCR

Total RNA was extracted from cultures grown in 75 mL culture flasks to approximately 90% confluence under proliferative conditions at 33 °C and after 14 and 30 days differentiation at 39 °C, using RNeasy kits (Qiagen). RNA yield was quantified using Versafluor (Biorad) and purified by DNase digestion. cDNA synthesis was carried out by oligo (dT) primed reverse transcription using M-MLV reverse transcriptase (RT, Stratagene). For each culture condition and tissue sample a negative control was prepared by carrying out the reaction in the absence of RT. In addition a 'mock' sample was prepared that had no mRNA added to the RT reaction.

Amplification of the sequences for potassium channel α-subunits was carried out using the following primer pairs (all 5′–3′; expected product sizes shown). Kv1.1, forward TCG ACC GCT CCA GGT CAC CC, reverse GTC GAT GCG GTG GAT GGT GC, 562 bp; Kv1.2, forward GCT ACC GGA GAC CCA GTG GA, reverse CCA CCA TGC ATG TCC TCA TT, 564 bp; Kv1.3, forward TCG AGA CGC AGC TCA AGA C, reverse ATA TTC GAA GAG CAG CCA, 334 bp; Kv1.5, forward GCC ATG ACC CTC AGA GGA GG, reverse GTG ATG GAG TGA TCC TGA GT, 275 bp; Kv1.6, forward GCG GCG GCG GCT GCT GTA, reverse GTT GGT CTC CAT GAG TCT CC, 422 bp; Kv2.1, forward AGG GAT CTC CTG AGA AGG CCA G, reverse GGC GGG CCC GGA ACT CTC, 397 bp; Kv2.2, forward GAG GTT AGC CAA AAA GAC TC, reverse TTG CAA AGG ACC ATG GGA AG, 524 bp; Kv3.1, forward CCA TGC CGG TGC CTG TCA TCG TGA, reverse TTC CTA CCT GCT CTG TTA ATT T, 225 bp; Kv3.2a, forward GCA AGC TCA CCT ACA TTT TG, reverse TCC ATC AGA AGC GCA CGT GT, 259 bp; GAPDH, forward, AACGGGAAGCCCATCACC reverse CAGCCTTGGCAG-CACCAG, 424 bp.

Amplification of the sequence for the HCN subunits was carried out using the following primer pairs (all 5′–3′; expected product sizes shown). HCN1 sense ACCTGCTACGCAATGTTTG, HCN1 antisense TCAGCTTCATTTCTTTACTGGA, 448 bp; HCN2 sense CGCATCTGTAACCTGATCA, HCN2 antisense GGCTGGAAGAC-CTCAAATT, 605 bp; HCN3 sense ATCGTGGTGGAGGAAGGTG, HCN3 antisense CTGCAGCATAGGGACCAGA, 383 bp; HCN4 sense GGTCAACAAATTCTCCCTAA, HCN4 antisense CAAT-GCGCACAGCCCTA, 455 bp; (Sartiani *et al.*, 2002).

Reactions were carried out with HotstarTaq (Qaigen). A step of 94 °C for 15 min was followed by 32 cycles (28 for GAPDH, 35 for HCN3, 40 for HCN1, 2 and 4) of 94 °C for 30 s, annealing at 58 °C (48 °C for Kv3.2a) for 30 s and extension at 72 °C for 30 s (all at 60 s for HCN1–4). A final step of 72 °C for 7 min was used at completion of the cycles. The number of cycles was chosen to ensure that amplification remained in the exponential phase at the end of the reaction by previous kinetic analysis, allowing a degree of quantification. PCR products were visualized by electrophoresis on 1% agarose gels stained with ethidium bromide. Amplification of the correct fragment was determined firstly by observation of product size, and subsequent cloning of the product and sequence analysis.

Each PCR reaction included RT-negative controls, a 'mock' control with no DNA or –RT sample, and positive controls from C57 mouse brain cDNA and genomic DNA. GAPDH primers were used as positive controls for cDNA presence/absence as appropriate and to provide an indication of amount of cDNA in each sample.

Cell transplantation into intact auditory nerves

All the animal experiments were conducted in accordance with the Guidelines for Animal Experiments at Kyoto University. Male Sprague–Dawley rats weighing 500–550 g each were anaesthetized by an intraperitoneal injection of ketamine (100 mg/mL; Sankyo Co., Tokyo, Japan) and xylazine (9 mg/mL; Bayer, Tokyo, Japan). After the rat was fixed in a small animal stereotactic frame (Model 900, David Kopf Instruments, Tujunga, CA, USA), right suboccipital craniectomy was performed with the aid of a surgical microscope and the seventh and eighth cranial nerve trunks were identified in the cerebellopontine angle cistern.

For cell transplantation, two different techniques were utilized. In technique 1 ($n = 8$), the cells were infused into the auditory nerve through a fused silica tube (the external and internal diameter, 107 and 40 μm, respectively) inserted into the cisternal portion of the auditory nerve in the cerebellopontine angle. The insertion site was covered by a layer of fibrin glue (Beriplast P, ZLB Behring) to prevent spillage of the transplanted cells and 2-μl portions of cell suspension (1×10^5 cell/μl) were infused into the auditory nerve trunk using a microinjector (Micro4, World Precision Instruments, Sarasota, FL, USA). Injection speed was 300 nL/min.

In technique 2 ($n = 6$), some auditory nerve tissue was deliberately removed in a piecemeal fashion from the internal auditory meatus near the brainstem. Step by step recordings were made to ensure that at least wave I of the auditory brainstem response (ABR) was preserved. With this procedure, a hole was created within the auditory nerve trunk in which the cells were transplanted using a fused silica tube. In two rats treated with technique 2, 4 μl of BD Matrigel Matrix High Concentration (HC)® (Nippon BD, Tokyo, Japan) was applied to plug the orifice of the hole. Fibrin glue alone was not always sufficient to secure the transplanted cells within the hole.

Auditory electrophysiology

ABRs were recorded between the base of the earlobe of the operative side (right) and the vertex with the ground electrode at the base of the forelimb. Click stimuli (90 dB sound pressure level) were presented to the right ear at a rate of 9.5 pulses/s through a tube earphone driven by a 100-μs rectangular pulse wave fed by a stimulator, and evoked potentials were amplified with a bandpass of 50 Hz to 3 kHz and were averaged using a processor (Synax 1100, NEC Medical Systems, Tokyo, Japan) with a sampling interval of 20 μs and 500 data points in each recording. The potentials to 100 successive clicks were averaged and stored in a computer (Sekiya *et al.*, 2000). During the first and second compression procedures, the compound action potentials (CAPs) were recorded between the tip of the compression-recording electrode and the vertex with the ground electrode placed at the base of the forelimb of the rat. For CAP recordings, the potentials from the nerve to five successive clicks were averaged and stored in a computer. This rate led to a continuous CAP recording rate of one potential every 2.4 s before the flat point. ABRs were recorded before and after cell transplantation and then immediately before killing the animals.

Immunocytochemistry

In preparation for immunocytochemistry each rat was placed in a state of deep anaesthesia and was perfused transaortically with 4% paraformaldehyde in 0.01 M phosphate-buffered saline (PBS) at pH 7.4. Three hours later, both temporal bones and the brain stem were removed en bloc. Both temporal bones were removed and decalcified with 10% ethylenediaminetetraacetic acid (EDTA) and HCl solution (pH 7.4) for 4–5 weeks at 4 °C. Serial 8 μm frozen sections of each temporal bone embedded in OCT compound (Sakura Finetechnical, Tokyo, Japan) were made. Midmodiolar sections included four good cross-sections of Rosenthal's canal (basal, lower middle, upper middle, and apical) and the widest part of the auditory nerve. These sections were mounted on glass slides, washed in PBS and dried in air at room temperature (RT) for 30 min. They were permeabilized and blocked with 10% goat serum in 0.2% Triton X-100 (Sigma) in PBS for 30 min. A primary antibody (anti-EGFP rabbit serum, ×500; Molecular Probes, Tokyo, Japan, diluted by 10% goat serum in 0.2% Triton X-100 PBS) was applied to the sections and incubated at 4 °C for 12 h followed by washing in 0.2% Triton X-100 PBS twice for 5 min each. A secondary antibody (Alexa Fluor 488 labelled anti-rabbit IgG goat antibody ×500, Molecular Probes, diluted by 10% goat serum in 0.2% Triton X-100 PBS) was applied to the sections at 4 °C for 6 h followed by washing in 0.2% Triton X-100/PBS twice for 5 min each. For nuclear staining, the sections were incubated in 4′-diamidino-2-phenylindole (DAPI) (0.1 μg/mL, Roche Molecular Biochemicals, Tokyo, Japan) solution at RT for 30 min. In several sections, nucleic acid dye (TOTO3, ×500, Molecular Probes) was applied for 15 min to stain nuclei for confocal microscopy. They were washed in 0.2% Triton/PBS twice for 5 min each. The sections were pre-equilibrated in the SlowFade Equilibration Buffer (Molecular Probes) for 30 min and mounted in SlowFade antifade reagent (Molecular Probes).

Mouse β3-tubulin polyclonal antibody (1 : 300; Covance Research Product, Berkeley, CA, USA) was used as the primary antibody to visualize neurites. Antibodies to cytokeratin (mouse monoclonal Ab, 1 : 500, Sigma #C2562), GFAP (mouse monoclonal antibody, 1 : 500, Sigma #G3893) and vimentin (mouse monoclonal Ab, 1 : 200, Boehringer Mannheim #814318) were used as markers for non-neuronal cells. For negative controls, primary antibody was omitted from the reaction series.

A fluorescence microscope system equipped with appropriate filters (Olympus BX50 + BX-FLA, Olympus, Tokyo, Japan) was used for observation. Samples were photographed with a digital camera (Olympus DP10). For confocal microscopy, a Leica TCS SP2 confocal laser scanning microscope (Leica Microsystems, Tokyo, Japan) was used. Images used for the figures were processed with Photoshop and Illustrator software programs (Adobe Systems, Mountain View, CA).

Results

Cell physiology and expression of ion channels

Cell lines such as VOT-N33 express different membrane conductances under differentiating conditions. We recorded these changes to determine how much functional differentiation was likely to have occurred at the point of transplantation and whether this was consistent with that expected from native spiral ganglion neurons. Under proliferating conditions relatively small, apparently instantaneous currents were generated in response to voltage steps from a holding potential of −64 mV (Fig. 1A and C). After 14 days under differentiating conditions most of the cells expressed larger, slowly activating

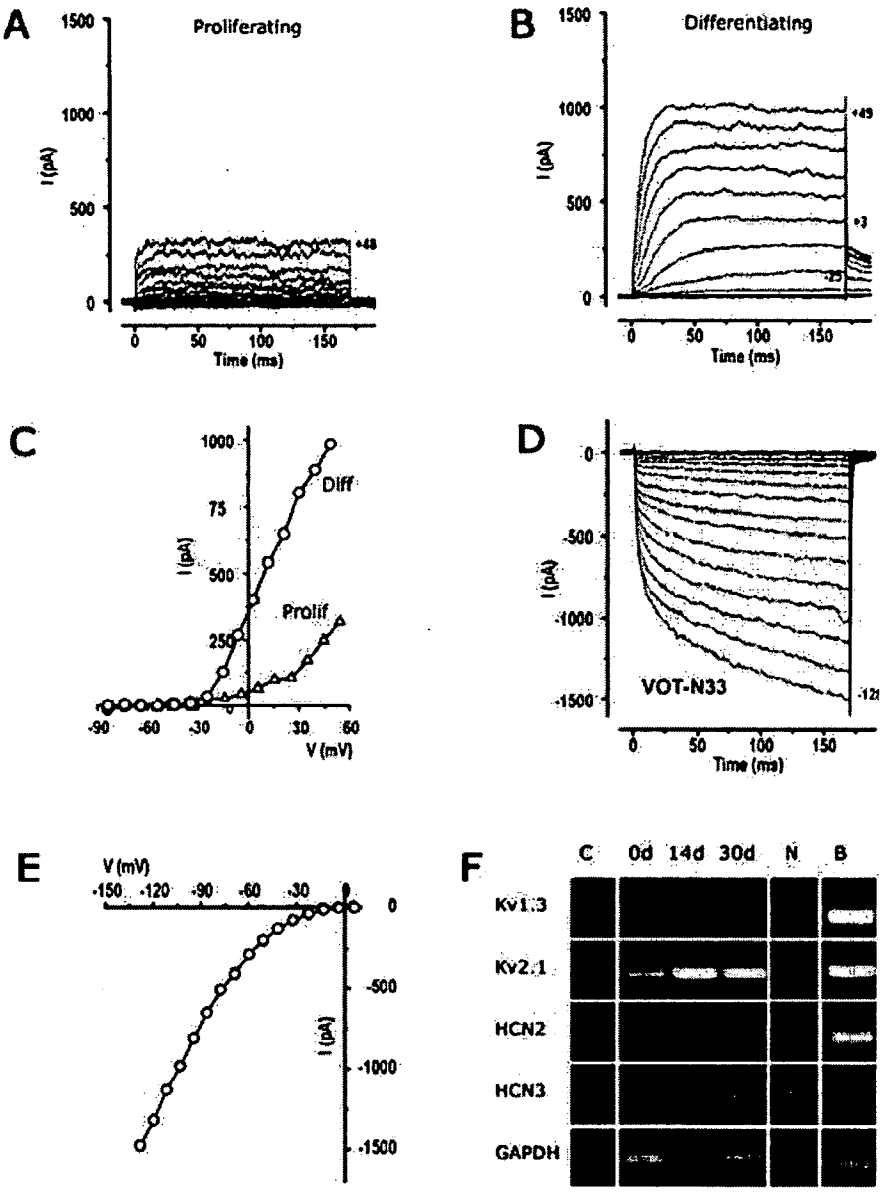

FIG. 1. Electrophysiology of VOT-N33 under proliferating and differentiating conditions. (A) Outward currents in proliferating cells in response to 10 mV voltage steps to between −80 mV and 64 mV from a nominal holding potential of −64 mV. (B) Outward currents as in A from a cell differentiated for 14 days. (C) Current–voltage curves corresponding to panels A and B. (D) Inward rectifier currents recorded under differentiating conditions in response to 10 mV steps from −130 mV to 20 mV. Subtracted leak conductance was 0.2 GΩ. (E) Current–voltage curve from the cell recordings shown in D. (F) RT-PCR for potassium channel subunits (Kv) and inward rectifier channel subunits (HCN) in VOT-N33, showing evidence for expression of Kv1.3, Kv 2.1, HCN2 and HCN3. All other subunits screened were negative. Samples are from cells grown under proliferating conditions (0 days) and under differentiating conditions for 14 and 30 days. GAPDH expression was used as a control and an indication of the relative amount of cDNA produced from each time point examined. Lane 'C' was a control with no mRNA, lane 'N' a control with no reverse transcriptase and lane 'B' was a positive control with cDNA from mouse brain.

outward currents (Fig. 1B and C). The instantaneous IV curve for cells under differentiating conditions showed a reversal potential of approximately −67 mV, suggesting that the conductances were mediated by potassium ions.

Inward currents were elicited using a series of voltage steps from a nominal −130 mV to +20 mV from holding potentials close the cell resting potential. When grown under proliferating conditions the cells expressed little or no inward current. However, at all time points examined during differentiation (6–34 days) some cells expressed a slowly activating inward current (Fig. 1D and E). This conductance was expressed in approximately half the cells examined with a mean amplitude of −985 ± 158 pA (n = 35) and a current density of −15.7 ± 4.1 mV. The mean resting membrane potential, Vm, was −14.6 ± 1.6 mV and the mean capacitance, Cm, was 59.1 ± 4.6 pF.

The recorded inward current showed characteristics of the mixed-cation conductance I_h previously identified in an immortalized cell line derived from the later E14 embryonic stage (Jagger *et al.*, 1999). It was blocked by 2 mM Cd^{2+} (n = 5, not shown), partially and reversibly blocked by 5 mM Cs^{+} (n = 3), and insensitive to 0.5 mM Ba^{2+} (n = 4). The current reversed at a relatively positive potential of

−5.9 ± 1.1 mV (n = 6), in close agreement with findings of Jagger *et al.* (1999), and consistent with a mixed ion current. In cells cultured with Neurobasal, B27 and FGF-2 we observed no additional currents to those described in serum. Despite expressing β3-tubulin and differentiating a bipolar phenotype we never observed the voltage-dependent sodium or calcium currents characteristic of mature neurons.

We screened VOT-N33 by RT-PCR for channel subunits that might underlie the outward rectifiers and I_h currents. The only voltage-gated potassium channel subunit expressed under differentiating conditions was Kv2.1, with evidence for low expression of Kv1.3 under proliferating conditions (Fig. 1F). We also looked for expression of the four subunits of the HCN family that might carry the I_h current. RT-PCR products of the predicted fragment size for mRNA for HCN2 and HCN3 were detected (Fig. 1F). HCN1 and HCN4 were absent. Expression levels for HCN2 were relatively constant during growth under both proliferating and differentiating conditions (14 and 30 days) whereas HCN3 was only expressed under differentiating conditions, with stronger expression after 30 days growth. As I_h was not recorded under proliferating conditions it may be dependent upon coexpression of HCN3.

Cell transplantation

The results following transplantation *in vivo* were derived from 14 rats, eight transplanted by technique 1 and six by technique 2 (Table 1). In one animal from each group we did not detect any transplanted cells. The areas in which cells were located at the end of the experiment were divided into four parts to show proximity to Rosenthal's canal in the cochlea and to the injection site (Fig. 2).

Cell migration after transplantation

Cells prepared for transplantation (Fig. 3A) were delivered to the cisternal part of the auditory nerve adjacent to the brainstem (area 3, Fig. 2) and were readily identified in subsequent histology by fluorescence microscopy. After 4 days many cells had migrated at least 1 mm along the nerve tract both peripherally, towards the organ of Corti, and centrally, towards the hindbrain (Fig. 3B). At this stage the cells were obviously aligned along the axis of the nerve but they resembled elongated, migratory fibroblasts and did not differentiate the typical morphology of a spiral ganglion neuron (Fig. 3C). In all of the subsequent histological analysis we did not find any cells outside the nerve tissue. No cells were observed in the cochlear duct or in Rosenthal's canal after 63 days, the longest period analysed during these experiments.

TABLE 1. Summary of results from transplanted animals

Technique and rat ID	Survival (days)	ABR retained?	Transplanted cells observed?	Cell processes observed?	Location to areas 1–4 (Fig. 6)
Technique 1					
(1) 05-10-21-3	7	Yes	Yes	Yes	1
(2) 05-11-18-1	10	Yes	Yes	Yes	2
(3) 05-9-9-3	10	Yes*	Yes	Yes	2–3
(4) 05-11-4-2	17	Yes	Yes	Yes	2
(5) 05-11-4-1	17	Yes	Yes	Yes	2
(6) 05-10-21-1	18	Yes	No	–	–
(7) 05-10-14-1	31	Yes	Yes	Yes	1
(8) 05-10-28-1	17	Yes	Yes	Yes	2
Technique 2					
(9) 05-6-10-1	4	No	Yes	Yes	1–4
(10) 06-1-6-3 (mgel)	39	No	No	–	–
(11) 06-2-3-2 (mgel)	47	No	Yes	Yes	2
(12) 06-2-3-1	47	No	Yes	Yes	3–4
(13) 06-1-20-1	63	No	Yes	Yes	4
(14) 06-1-6-4	39	No	Yes	Yes	3

*ABR retained after cell transplantation, but not available prior to killing.

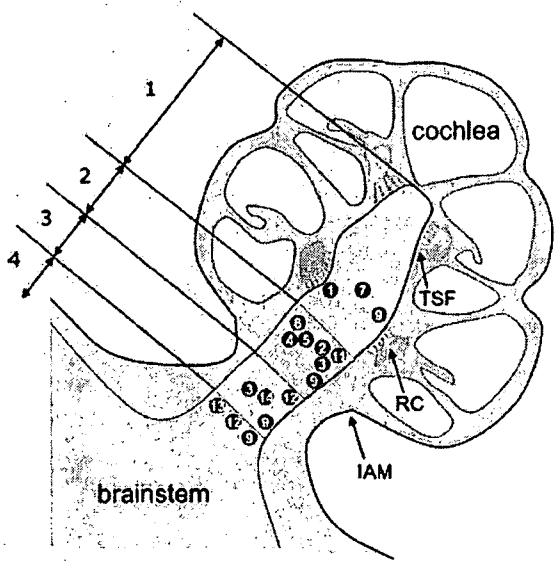

FIG. 2. Diagram taken from a mid-modiolar section of the cochlea to show the locations of transplanted cells with respect to Rosenthal's canal. The numbered areas describe the distal portion of the auditory nerve (1), the internal auditory meatus distal to the injection site (2), the injection site (3) and a region central to the injection site towards the brainstem (4). Note that the relative proportions of dendritic to axonal processes would be very different for cells located in different areas. A group of cells located in area 4 would also have dendrites of very different lengths if they projected throughout the length of the cochlea.

Cell survival and differentiation after transplantation

A week to 10 days after transplantation groups of transplanted cells were found with a more restricted distribution (Fig. 4A). These cells showed significant signs of differentiation and more closely resembled spiral ganglion neurons (Fig. 4B). They were spherical with a centrally located nucleus and were organized into what appeared to be ectopic ganglia. Despite extensive migration along the nerve, transplanted cells were not distributed evenly and few individual cells existed in isolation. This applied to all animals analysed from 7 to 63 days after transplantation. Given their similarity to endogenous spiral ganglion neurons we measured the transverse diameter of the cell bodies and the areas of sectioned profiles of the cell bodies and their nuclei. Endogenous spiral ganglion neuron bodies were slightly larger in the basal turn than in the middle or apical turns ($P < 0.001$, Fig. 5A and B) but together they averaged 12.1 ± 1.4 μm. All transplanted cells were significantly bigger at 18.7 ± 3.4 μm (Fig. 5A and C). Independent measures of the cross-sectional areas of the cell bodies were also significantly higher for transplanted cells, as expected from the diameter measurements ($P < 0.0001$, Fig. 5D), and the nuclear sections were also bigger ($P < 0.0001$, Fig. 5E).

Serial sections taken from animal number 8 (17 days after transplantation) allowed us to estimate the number of transplanted cells that survived. Alternate sections, 8-μm thick, were taken to avoid double counting and in a total of eight separate sections there were 657 cells

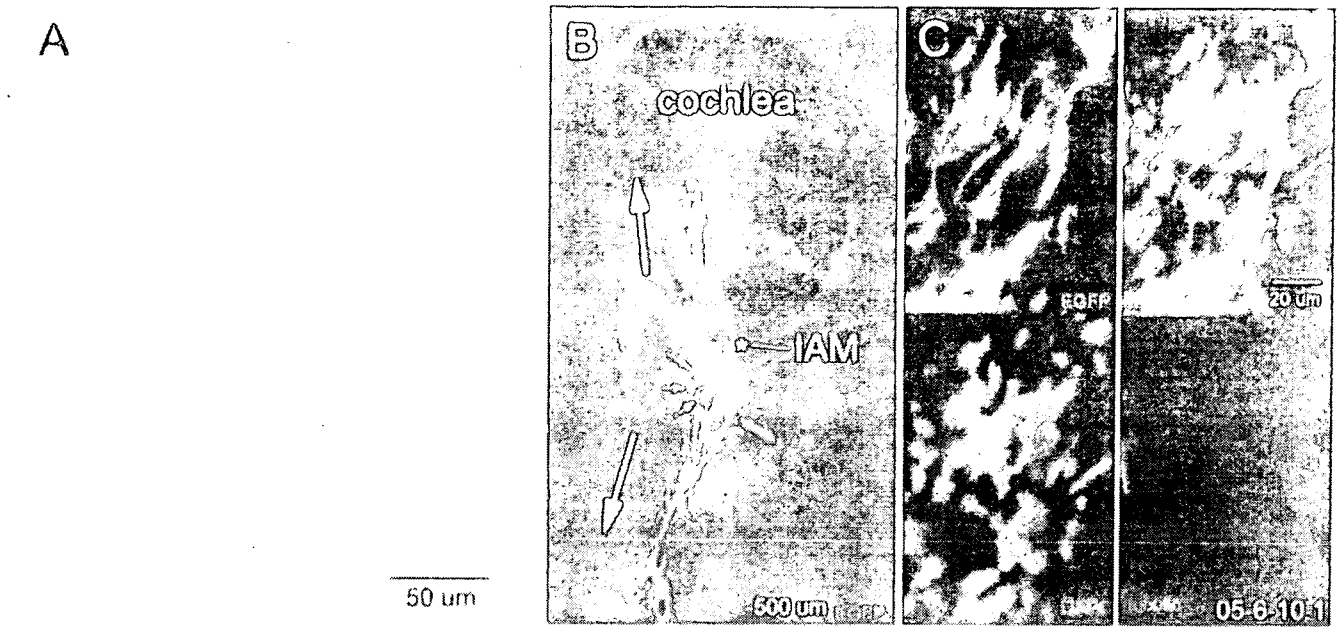

FIG. 3. (A) N33 cells under proliferating conditions *in vitro* before transplantation. They resembled motile, elongated fibroblasts. (B) Whole cochlear section from animal 9 (Table 1) killed 4 days after transplantation. Transplanted cells migrated from the transplantation site bi-directionally (large arrows) from the transplanted site (small arrows). Asterisk indicates the position of the internal auditory meatus (IAM). (C) A higher magnification image from B, showing that transplanted cells were aligned within the host nerve tissue but remained fibroblastic in morphology. They did not label with anti-β3-tubulin.

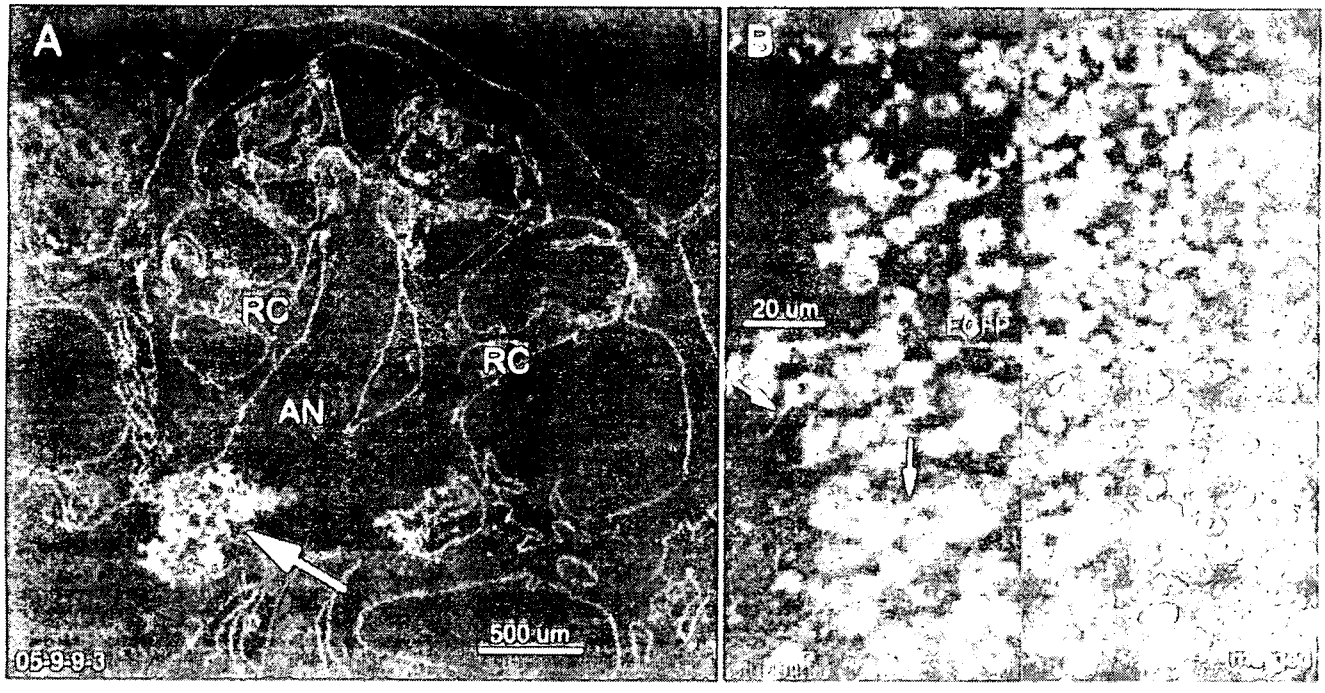

FIG. 4. (A) Transplanted cells labelled with EGFP in area 2–3 of an animal 3 (Table 1) examined after 10 days. The cells aggregated into a group and few isolated cells were visible. AN, auditory nerve; RC, Rosenthal's canal. (B) A higher magnification from A showing that transplanted cells (top left) were strikingly different to those cultured *in vitro* or examined after only 4 days (Fig. 3). They were morphologically similar to endogenous spiral ganglion neurons, expressed β3-tubulin and extended neuritic projections centrally (arrows in bottom panels). They were surrounded by many other cells of the endogenous neural tissue (top right).

that expressed EGFP. This number includes a correction for cell diameter and section thickness (Abercrombie, 1946). The maximum number of cells in a single section was 120. We were unable to obtain full serial sections for all animals but the maximum number of cells in single, mid-modiolar sections was 199 (animal number 3, 10 days), 81 (animal number 4, 17 days), 100 (animal number 5, 17 days) and 101 (animal number 11, 47 days). This data suggests a survival rate of more than 400 cells resembling ganglion cells per animal.

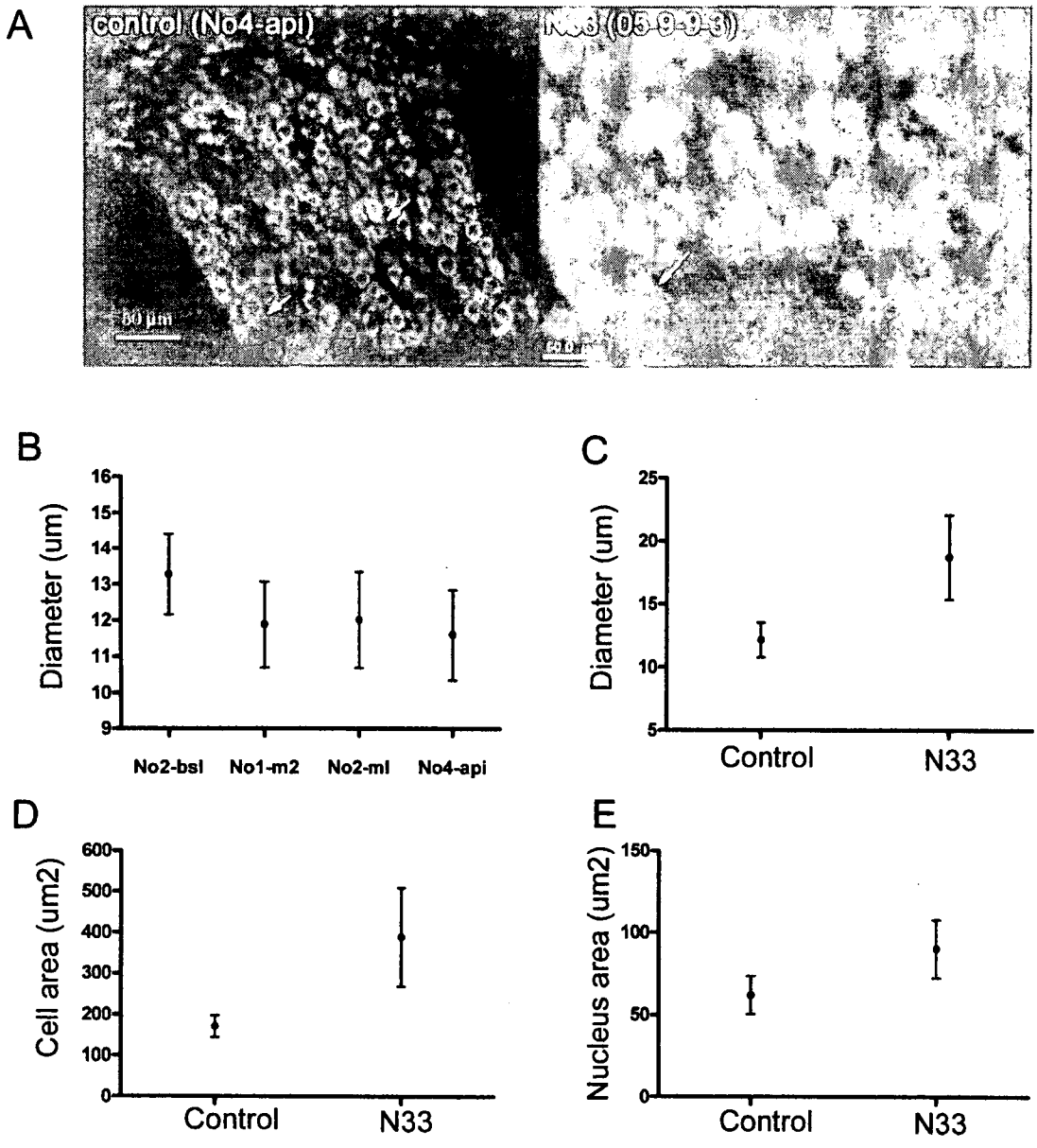

FIG. 5. (A) Control (left) and transplanted N33 cells (right). Note the bigger size of the transplanted cells as statistically verified in B to E. Also note that in the controls, the typical bipolar morphology of the spiral ganglion neurons was not readily visible with labelling for β3-tubulin. The arrows indicate central projections in both panels. (B–E) Measurements of cell diameter and cross-sectional area for cell bodies of transplanted cells and endogenous spiral ganglion neurons. (B) Mean and standard deviation for endogenous spiral ganglion cell diameter at right angles to the neural axis for cells in the basal (No2-bsl, $n = 27$), lower middle (No1-m2, $n = 32$), upper middle (No2-m1, $n = 31$) and apical (No4-api, $n = 51$) regions of the cochlea. Data was analysed by analysis of variance with Tukey's multiple comparison. (C) Comparison between the mean and standard deviation for cell diameter between endogenous cells (control $n = 141$) and transplanted cells (N33 $n = 182$). Transplanted cells were significantly bigger (t-test, $P < 0.001$). (D) Comparison between the mean and standard deviation for cell cross-sectional area between endogenous cells (control $n = 117$) and transplanted cells (N33 $n = 134$). Transplanted cells were significantly bigger (t-test, $P < 0.0001$). (E) Comparison between the mean and standard deviation for nuclear cross-sectional area between endogenous cells (control $n = 72$) and transplanted cells (N33 $n = 51$). Nuclei in transplanted cells were significantly bigger (t-test, $P < 0.0001$).

There were no obvious differences in the morphology of the transplanted cell bodies from 7 to 63 days but there was evidence for growth of neuron-like projections in all animals in which transplanted cells were found (Table 1). The cells appeared to differentiate a bipolar morphology with both central and peripheral projections. Peripheral projections with a 'dendritic' orientation were most clearly observed when cells were located in area 1 (Fig. 6A). Some of these projections were at least 60-µm long, the actual length being hard to measure in mid-modiolar sections of this type. The EGFP label was much harder to trace than the immunolabel for β3-tubulin (Fig. 6A) and it was difficult to track dendrites for their full length. The same problem applied to projections from mature, endogenous neurons (Fig. 5A), for which it should be noted that they express β3-tubulin only in the axons and not in the dendrites. Central projections with an 'axonal' orientation were observed as early as 7–10 days after transplantation (Fig. 6B). In all cases the transplanted cells expressed both EGFP and β3-tubulin (Figs 4–6). None labelled with antibodies directed against cytokeratins, vimentin

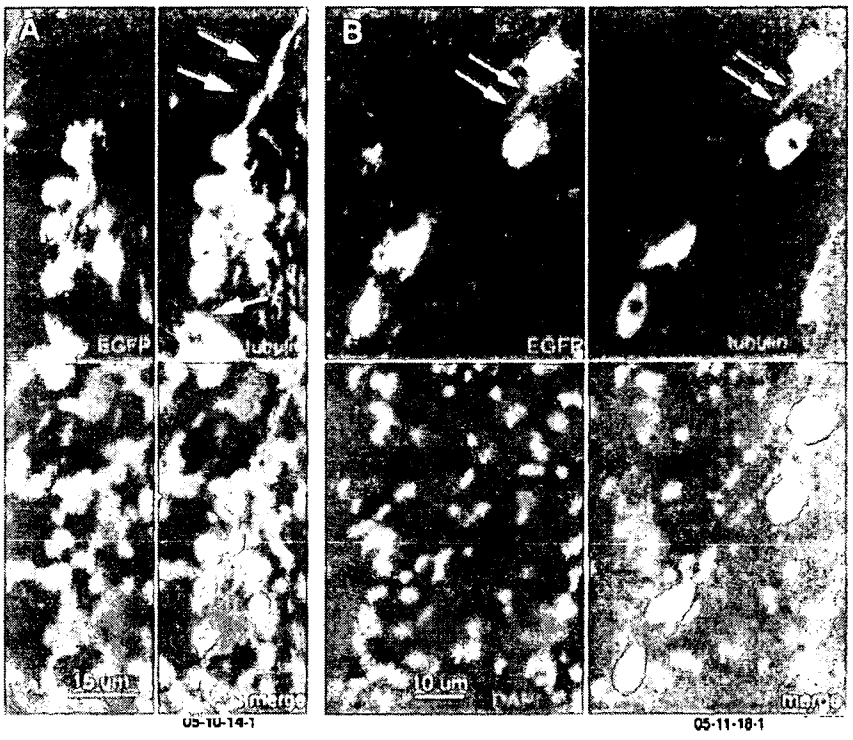

FIG. 6. (A) Transplanted cells labelled with EGFP in area 1 of animal 7 (Table 1) examined after 31 days. The cells aggregated into a small group, which were morphologically similar to endogenous spiral ganglion neurons, expressed β3-tubulin and extended neuritic projections peripherally (arrows in top right panel). They were surrounded by many other cells from the endogenous neural tissue. (B) Transplanted cells labelled with EGFP in area 2 of animal 2 (Table 1) examined after 10 days. This image shows projections directed centrally towards the brainstem (arrows).

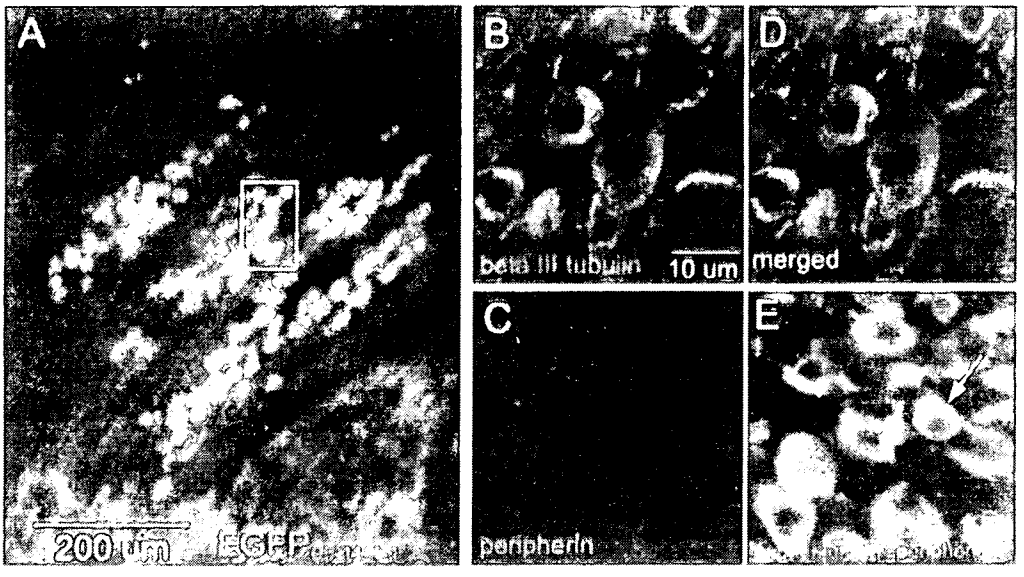

FIG. 7. (A) Transplanted cells within area 2 of animal 5 examined 17 days after transplantation (Table 1). In this case the cells were not only aggregated into groups but also aligned in irregular rows along the axis of the nerve. The rectangular area is enlarged in B–D. (B–E) Transplanted cells were labelled with β3-tubulin antibody (B) but not with peripherin antibody (C). The same antibodies applied to endogenous spiral ganglion neurons in Rosenthal's canal of the same animal showed labelling for peripherin (E, arrow), which is normally expressed in type II but not type I spiral ganglion neurons.

or glial fibrillary acidic protein (not shown), which suggested that they had retained their original neuronal identity and had not adopted epithelial, mesenchymal or glial cell phenotypes, respectively, *in vivo*. Furthermore, none expressed peripherin (Fig. 7), which is normally expressed in type 2 but not type 1 spiral ganglion neurons (Dau & Wenthold, 1989).

These observations indicated that VOT-N33 cells were able to migrate along the auditory nerve, survive more than 2 months and

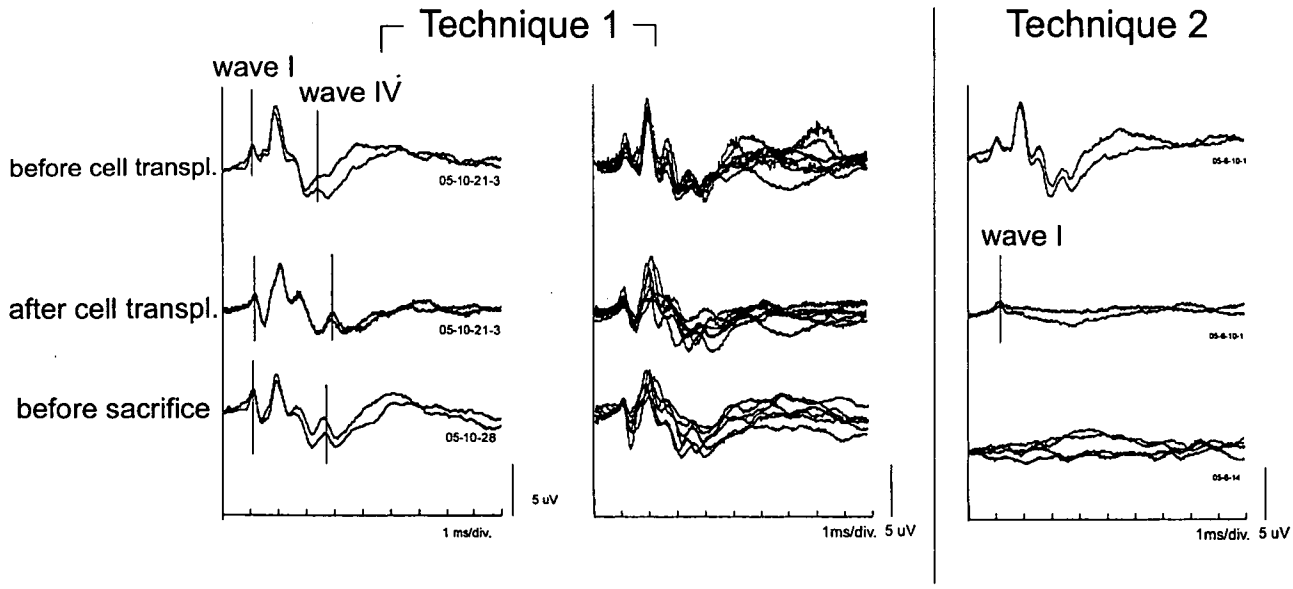

FIG. 8. ABR recordings from animals treated by technique 1 (left and centre panels) and technique 2 (right). Technique 1 preserved the ABRs more effectively and they were not degraded as a result of the presence of transplanted cells. Technique 2 shows a loss of the ABR that was not recovered after transplantation for up to 63 days. The centre panel shows the superimposed ABRs from all rats injected using technique 1.

differentiate with a morphology similar to that of native spiral ganglion neurons. There was no sign of tumour formation in any of the experimental animals.

ABR recordings before and after cell transplantation

In the rats transplanted by technique 1, where cells were inserted through a fused silica tube, each peak of the ABR was preserved (Fig. 8, left and centre panels). In some cases, interpeak latencies were improved by the time of the temporal bone removal. Moreover, in several rats, the interpeak latency between wave I and IV was shortened in comparison with that in the pre-cell transplantation period. In the rats transplanted by technique 2 the ABR deteriorated considerably after removal of some auditory nerve tissue at the internal auditory meatus (Fig. 8, right panel). However, wave I of the ABR was always maintained, indicating that the blood flow to the cochlea was not damaged. Technique 1 maintained an ABR that did not suffer further degradation as a result of either the injection or long-term effects of transplanted cells (Fig. 8, left and centre panels). Functional recovery was not observed in any experimental animal.

Discussion

We have shown that conditionally immortal cells derived from embryonic mouse auditory neuroblasts can survive and differentiate following transplantation to the rat auditory nerve *in vivo*. With appropriate surgery the transplanted cells caused minimal degradation of the ABR for up to 63 days post-transplantation. This demonstration that the donor cells were incorporated without large scale functional damage to the host is a key requisite for further studies on cell transplantation.

A model for cell transplantation

Our experimental approach allows us to control key variables in transplantation experiments. The differentiation state of donor cells can be defined and controlled relatively accurately prior to injection and cells can be injected into a reproducible location in the auditory nerve (Sekiya *et al.*, 2000). Conditionally immortal cell lines offer a number of advantages over other sources of cells, including embryonic and tissue-specific stem cells, and have been used successfully for structural and functional recovery in the mammalian retina (Lund *et al.*, 2001a; Lund *et al.*, 2001b), hippocampus (Renfranz *et al.*, 1991; Virley *et al.*, 1999) and other regions of the brain (Kim, 2004; Ryu *et al.*, 2005). A similar technology applied to human tissue-specific stem cells is now being tested in preclinical trials for treatment of stroke (Pollock *et al.*, 2006). One of the major technical advantages is that cells can be produced, characterized and controlled relatively easily without the need to derive material repeatedly from primary tissue. A further advantage of our model is that the donor cells are derived from embryonic cochlear neuroblasts. Such cells do not have the plasticity of stem cells but this can be an asset in terms of targeting specific cell populations with a greater degree of control. In our experiments all labelled donor cells adopted a neuronal phenotype and did not express markers for epithelial, mesenchymal or glial cells. Our model should help us to develop proof-of-principle for the use of conditionally immortal cell lines in the ear and should help us to objectively analyse the key conditions for successful functional integration.

Cell differentiation prior to transplantation

The electrophysiology revealed the immaturity of VOT-N33 cells as neurons. The cells did not express the voltage-gated sodium or calcium channels that are normally observed in mature neurons. The outward current is most likely to be carried by potassium and is a common feature of cells during early stages of differentiation. Previous analysis by RT-PCR suggests that KCNQ3, a neuronal potassium channel subunit (Jentsch, 2000), is expressed in VOT-N33 (Lawoko-Kerali *et al.*, 2004). In conjunction with the voltage-gated subunit Kv2.1 it might underlie the delayed rectifier. The presence of the mixed-cation current I_h and the HCN2 and HCN3 subunits is

expected in normal spiral ganglion neuroblasts. I_h currents have been recorded from type-I spiral ganglion neurons (Mo & Davis, 1997; Szabo *et al.*, 2002). The HCN subunits are widely expressed in neuronal tissue (Vincent *et al.*, 2002) and HCN2 is expressed in rat auditory brainstem nuclei and cochlear pyramidal cells (Pal *et al.*, 2003; Koch *et al.*, 2004). We conclude that the membrane properties recorded from VOT-N33 are consistent with their identity as spiral ganglion neurons at a very early stage of differentiation.

Migration, aggregation and differentiation of transplanted cells

If donor cells are not delivered with precision to the target site during surgery then they must be able to migrate to it from the delivery site. The migratory behaviour of immortal cell lines has previously been demonstrated in the location and repair of lesions in the central nervous system (Martinez-Serrano & Bjorklund, 1997; Gray *et al.*, 1999). VOT-N33 was originally selected to represent auditory neuroblasts newly delaminated from the otic vesicle (Nicholl *et al.*, 2005). During normal development, the native cells subsequently migrate through the periotic mesenchyme, aggregate to form the cochlear-vestibular ganglion and differentiate to form bipolar sensory neurons that project to the cochlea and cochlear nuclei (Rubel & Fritzsch, 2002; Alsina *et al.*, 2004). There is a relatively long period of maturation but the key parts of this process take 4–5 days, from E9–E14 (Fig. 9A). This behaviour was reflected by VOT-N33 cells following transplantation (Fig. 9B). The cells migrated along the auditory nerve during the first 4 days. Although individual cells may have continued to move through the host tissue there was no evidence in any animal examined thereafter, from 7 to 63 days, for migration any further from the injection site. This short period of migration was similar to that of normal neuroblasts despite the substantial differences between the cellular environment of embryonic periotic mesenchyme and the adult auditory nerve tract. The limits to migration might be purely a function of space as embryonic stem cells migrated further along the auditory nerve following nerve degeneration induced by compression (Sekiya *et al.*, 2006). Alternatively, they may reflect an inherent property of the cell line. Most transplanted cells remained within the neural tissue, suggesting that there may be attractive forces within the nerve or repulsive forces in the surrounding tissue, as observed from experiments with VOT-N33 *in vitro* (Nicholl *et al.*, 2005).

A further similarity to the normal behaviour of neuroblasts was the aggregation of transplanted cells into ectopic 'ganglia'. Relatively few isolated cells were observed. This behaviour suggests that the cells supported each other, possibly by secreting local soluble factors or by expressing cell surface molecules that stimulate aggregation and differentiation. During differentiation *in vitro* the cell projections adhere to each other to form small aggregates and bundles (Nicholl *et al.*, 2005). In our experiments the cells aggregated within the nerve trunk either up or down stream from the injection site rather than within or nearby Rosenthal's Canal. The barrier to cell migration into Rosenthal's canal could be more a function of physical than biochemical forces because the donor cells would be too large to pass through the tractus spiralis foraminosus (Fig. 2). This issue may be resolved following tissue degeneration because embryonic stem cells delivered to the nerve trunk following denervation with ouabain did project through the canal and to the organ of Corti (Corrales *et al.*, 2006).

The morphological differentiation of transplanted cells following injection was striking and again consistent with the behaviour of native neuroblasts. Transplanted cells appeared to differentiate between 4 and 7 days after injection, adopting the characteristic morphology of spiral ganglion neurons. Their larger cell bodies and nuclei may reflect the active protein synthesis and growth that should accompany extension of dendrites and axons. They extended bipolar, neuritic projections along the neuronal axis and both expressed β3-tubulin, a pattern that is consistent with native neurons in the embryonic and early postnatal cochlea. In normal adult tissue the dendrites do not express β3-tubulin (Jensen-Smith *et al.*, 2003) but there is evidence from other types of neuron for increased expression of β3-tubulin during regeneration (Havercroft & Cleveland, 1984; Moskowitz & Oblinger, 1995; Stone & Rubel, 2000).

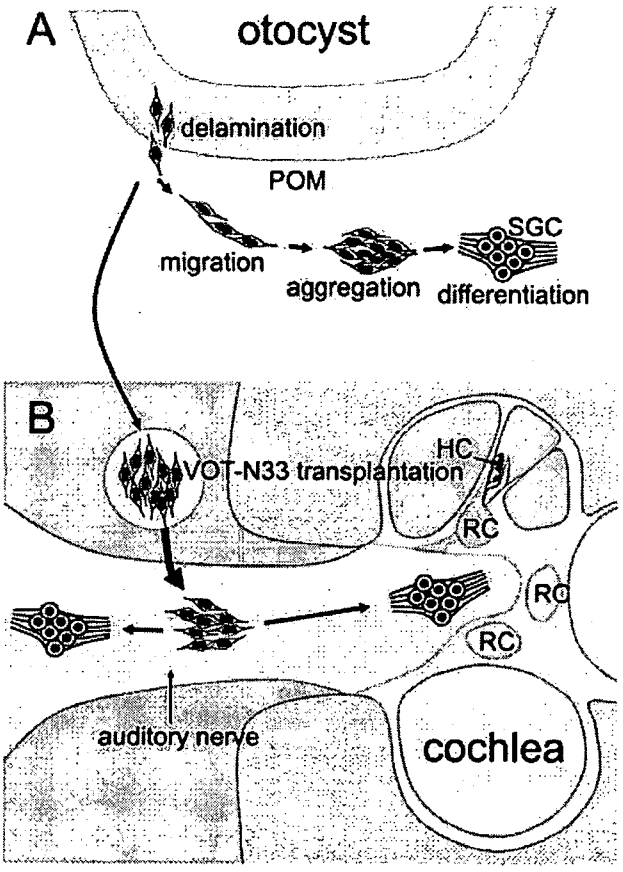

FIG. 9. (A) During normal development, sensory neuroblasts delaminate from the otocyst epithelium and migrate through the periotic mesenchyme (POM). During this phase there is a period of proliferation called transit amplification. The cells then aggregate and start to differentiate. The process occurs over a period of approximately 4 days and migration occurs over a distance of up to 500 μm. (B) Transplanted cells recapitulate the process of migration, aggregation and morphological differentiation in the adult rat auditory nerve tract but do not locate to Rosenthal's canal (RC), from where the spiral ganglion cells (SGC) would normally project dendrites to the hair cells (HC).

Maintenance of the ABR

Retaining a strong ABR following surgery and after longer periods of recovery with injected cells is an important result and may not apply equally to all types of donor cell. Survival rates following transplantation are usually very low, which means that the host tissue must process the debris from many thousands of cells, in this case up to 2×10^5 cells, without compromising function. The deterioration of

the ABR with technique 2 was caused by the removal of auditory nerve tissue at the internal auditory meatus. In contrast, the ABR changes observed in the rats where technique 1 was used were minimal. The insertion of a fused silica tube appeared to reduce the surgical injury to the auditory nerve. The subsequent activity of the donor cells might have caused slowing of impulse conduction but this recovered gradually in accordance with cell migration away from the transplantation site. In several rats where technique 1 was used, the interpeak latencies between wave I and IV immediately before killing the animals were shortened in comparison with those before craniectomy. The precise reasons for this phenomenon are not clear. We did not observe functional recovery in those animals that suffered surgical damage to the auditory nerve but our results suggest refinements for an experimental approach that could yield more successful incorporation in the future. BD Matrigel Matrix High Concentration (HC)® is a solubilized basement membrane preparation extracted from a tumour rich in extracellular matrix proteins. Its major component is laminin, followed by collagen IV, heparan sulphate proteoglycans, and entactin (Kleinman *et al.*, 1982). It becomes a gel at room temperature due to its high protein concentration and is very sticky to the intracranial tissue. When we applied it topically in the cerebellar-pontine angle as plugging material we successfully secured cells within the transplantation site. The laminin may subsequently influence cell migration and differentiation (Costa *et al.*, 2002; Tardy, 2002), in which context it deserves further study.

Acknowledgements

The authors are supported equally by the Japanese Ministry of Education, Culture, Sports, Science, and Technology, the Colt Foundation (RH) and Deafness Research UK. We thank Drs Makoto Miura, Takayuki Nakagawa and Walter Marcotti for their critical discussions and also Ms. Yoko Nishiyama, Akemi Saito, Keiko Nishio for their technical expertise.

Abbreviations

ABR, auditory brainstem response; CAP, compound action potential; EGFP, enhanced green fluorescent protein.

References

Abercrombie, M. (1946) Estimation of nuclear population from microtome sections. *Anat. Record*, **94**, 239–247.

Alsina, B., Abello, G., Ulloa, E., Henrique, D., Pujades, C. & Giraldez, F. (2004) FGF signaling is required for determination of otic neuroblasts in the chick embryo. *Dev. Biol.*, **267**, 119–134.

Altschuler, R.A., Cho, Y., Ylikoski, J., Pirvola, U., Magal, E. & Miller, J.M. (1999) Rescue and regrowth of sensory nerves following deafferentation by neurotrophic factors. *Ann. NY Acad. Sci.*, **884**, 305–311.

Corrales, C.E., Pan, L., Li, H., Liberman, M.C., Heller, S. & Edge, A.S. (2006) Engraftment and differentiation of embryonic stem cell-derived neural progenitor cells in the cochlear nerve trunk: Growth of processes into the organ of corti. *J. Neurobiol.*, **66**, 1489–1500.

Costa, S., Planchenault, T., Charriere-Bertrand, C., Mouchel, Y., Fages, C., Juliano, S., Lefrancois, T., Barlovatz-Meimon, G. & Tardy, M. (2002) Astroglial permissivity for neuritic outgrowth in neuron-astrocyte cocultures depends on regulation of laminin bioavailability. *Glia*, **37**, 105–113.

Dau, J. & Wenthold, R.J. (1989) Immunocytochemical localization of neurofilament subunits in the spiral ganglion of normal and neomycin-treated guinea pigs. *Hear. Res.*, **42**, 253–263.

Gray, J.A., Hodges, H. & Sinden, J. (1999) Prospects for the clinical application of neural transplantation with the use of conditionally immortalized neuroepithelial stem cells. *Philos. Trans. R. Soc. Lond. B Biol. Sci.*, **354**, 1407–1421.

Hakuba, N., Hata, R., Morizane, I., Feng, G., Shimizu, Y., Fujita, K., Yoshida, T., Sakanaka, M. & Gyo, K. (2005) Neural stem cells suppress the hearing threshold shift caused by cochlear ischemia. *Neuroreport*, **16**, 1545–1549.

Havercroft, J.C. & Cleveland, D.W. (1984) Programmed expression of beta-tubulin genes during development and differentiation of the chicken. *J. Cell Biol.*, **99**, 1927–1935.

Holley, M.C. (2005) Keynote review: The auditory system, hearing loss and potential targets for drug development. *Drug Discov. Today*, **10**, 1269–1282.

Hu, Z., Ulfendahl, M. & Olivius, N.P. (2004) Central migration of neuronal tissue and embryonic stem cells following transplantation along the adult auditory nerve. *Brain Res.*, **1026**, 68–73.

Hu, Z., Wei, D., Johansson, C.B., Holmstrom, N., Duan, M., Frisen, J. & Ulfendahl, M. (2005) Survival and neural differentiation of adult neural stem cells transplanted into the mature inner ear. *Exp. Cell Res.*, **302**, 40–47.

Iguchi, F., Nakagawa, T., Tateya, I., Kim, T.S., Endo, T., Taniguchi, Z., Naito, Y. & Ito, J. (2003) Trophic support of mouse inner ear by neural stem cell transplantation. *Neuroreport*, **14**, 77–80.

Ito, J., Murata, M. & Kawaguchi, S. (2001) Regeneration and recovery of the hearing function of the central auditory pathway by transplants of embryonic brain tissue in adult rats. *Exp. Neurol.*, **169**, 30–35.

Izumikawa, M., Minoda, R., Kawamoto, K., Abrashkin, K.A., Swiderski, D.L., Dolan, D.F., Brough, D.E. & Raphael, Y. (2005) Auditory hair cell replacement and hearing improvement by Atoh1 gene therapy in deaf mammals. *Nature Med.*, **11**, 271–276.

Jagger, D.J., Holley, M.C. & Ashmore, J.F. (1999) Ionic currents expressed in a cell line derived from the organ of Corti of the Immortomouse. *Pflugers Arch.*, **438**, 8–14.

Jensen-Smith, H.C., Eley, J., Steyger, P.S., Luduena, R.F. & Hallworth, R. (2003) Cell type-specific reduction of beta tubulin isotypes synthesized in the developing gerbil organ of Corti. *J. Neurocytol.*, **32**, 185–197.

Jentsch, T.J. (2000) Neuronal KCNQ potassium channels: physiology and role in disease. *Nature Rev. Neurosci.*, **1**, 21–30.

Kim, S.U. (2004) Human neural stem cells genetically modified for brain repair in neurological disorders. *Neuropathology*, **24**, 159–171.

Kleinman, H.K., McGarvey, M.L., Liotta, L.A., Robey, P.G., Tryggvason, K. & Martin, G.R. (1982) Isolation and characterization of type IV procollagen, laminin, and heparan sulfate proteoglycan from the EHS sarcoma. *Biochemistry*, **21**, 6188–6193.

Koch, U., Braun, M., Kapfer, C. & Grothe, B. (2004) Distribution of HCN1 and HCN2 in rat auditory brainstem nuclei. *Eur. J. Neurosci.*, **20**, 79–91.

Kopke, R., Staecker, H., Lefebvre, P., Malgrange, B., Moonen, G., Ruben, R.J. & Van de Water, T.R. (1996) Effect of neurotrophic factors on the inner ear: clinical implications. *Acta Otolaryngol.*, **116**, 248–252.

Lang, H., Schulte, B.A. & Schmiedt, R.A. (2005) Ouabain induces apoptotic cell death in type i spiral ganglion neurons, but not Type II neurons. *J. Assoc. Res. Otolaryngol.*, **6**, 63–74.

Lawoko-Kerali, G., Milo, M., Davies, D., Halsall, A., Helyer, R., Johnson, C.M., Rivolta, M.N., Tones, M.A. & Holley, M.C. (2004) Ventral otic cell lines as developmental models of auditory epithelial and neural precursors. *Dev. Dyn.*, **231**, 801–814.

Li, H., Corrales, C.E., Edge, A. & Heller, S. (2004) Stem cells as therapy for hearing loss. *Trends Mol. Med.*, **10**, 309–315.

Lindvall, O., Kokaia, Z. & Martinez-Serrano, A. (2004) Stem cell therapy for human neurodegenerative disorders-how to make it work. *Nature Med.*, **10** (Suppl.), S42–S50.

Lund, R.D., Adamson, P., Sauve, Y., Keegan, D.J., Girman, S.V., Wang, S., Winton, H., Kanuga, N., Kwan, A.S., Beauchene, L., Zerbib, A., Hetherington, L., Couraud, P.O., Coffey, P. & Greenwood, J. (2001a) Subretinal transplantation of genetically modified human cell lines attenuates loss of visual function in dystrophic rats. *Proc. Natl Acad. Sci. USA*, **98**, 9942–9947.

Lund, R.D., Kwan, A.S., Keegan, D.J., Sauve, Y., Coffey, P.J. & Lawrence, J.M. (2001b) Cell transplantation as a treatment for retinal disease. *Prog. Retin. Eye Res.*, **20**, 415–449.

Martinez-Serrano, A. & Bjorklund, A. (1997) Immortalized neural progenitor cells for CNS gene transfer and repair. *TINS*, **20**, 530–538.

Mo, Z.L. & Davis, R.L. (1997) Heterogeneous voltage dependence of inward rectifier currents in spiral ganglion neurons. *J. Neurophysiol.*, **78**, 3019–3027.

Moskowitz, P.F. & Oblinger, M.M. (1995) Sensory neurons selectively upregulate synthesis and transport of the beta III-tubulin protein during axonal regeneration. *J. Neurosci.*, **15**, 1545–1555.

Naito, Y., Nakamura, T., Nakagawa, T., Iguchi, F., Endo, T., Fujino, K., Kim, T.S., Hiratsuka, Y., Tamura, T., Kanemaru, S., Shimizu, Y. & Ito, J. (2004) Transplantation of bone marrow stromal cells into the cochlea of chinchillas. *Neuroreport*, **15**, 1–4.

Nicholl, A.J., Kneebone, A., Davies, D., Cacciabue-Rivolta, D.I., Rivolta, M.N., Coffey, P. & Holley, M.C. (2005) Differentiation of an auditory neuronal cell line suitable for cell transplantation. *Eur. J. Neurosci.*, **22**, 343–353.